

EFFECT OF GEOTHERMAL DRAWDOWN ON SUSTAINABLE DEVELOPMENT, NEWCASTLE AREA, IRON COUNTY, UTAH

by
Robert E. Blackett, Howard P. Ross, and Craig B. Forster



Commercial greenhouses began in the early 1980s, and by 1988 three greenhouse complexes were producing tropical plants and vegetables for sale. In 1993 a California-based company purchased land, drilled new wells, and began construction of a geothermally heated greenhouse development.



CIRCULAR 97
UTAH GEOLOGICAL SURVEY
a division of
UTAH DEPARTMENT OF NATURAL RESOURCES

1997



EFFECT OF GEOTHERMAL DRAWDOWN ON SUSTAINABLE DEVELOPMENT, NEWCASTLE AREA, IRON COUNTY, UTAH

by
Robert E. Blackett, Howard P. Ross, and Craig B. Forster



Commercial greenhouses began in the early 1980s, and by 1988 three greenhouse complexes were producing tropical plants and vegetables for sale. In 1993 a California-based company purchased land, drilled new wells, and began construction of a geothermally heated greenhouse development.



CIRCULAR 97
UTAH GEOLOGICAL SURVEY
a division of
UTAH DEPARTMENT OF NATURAL RESOURCES

1997



ISBN 1-55791-609-8

STATE OF UTAH

Michael O. Leavitt, Governor

DEPARTMENT OF NATURAL RESOURCES

Ted Stewart, Executive Director

UTAH GEOLOGICAL SURVEY

M. Lee Allison, Director

UGS Board

Member	Representing
Russell C. Babcock, Jr. (Chairman)	Mineral Industry
D. Cary Smith	Mineral Industry
Craig Nelson	Civil Engineering
E.H. Deedee O'Brien	Public-at-Large
C. William Berge	Mineral Industry
Jerry Golden	Mineral Industry
Richard R. Kennedy	Economics-Business/Scientific
David Terry, Director, Trust Lands Administration	<i>Ex officio member</i>

UTAH GEOLOGICAL SURVEY

The **UTAH GEOLOGICAL SURVEY** is organized into five geologic programs with Administration, Editorial, and Computer Resources providing necessary support to the programs. The **ECONOMIC GEOLOGY PROGRAM** undertakes studies to identify coal, geothermal, uranium, hydrocarbon, and industrial and metallic resources; initiates detailed studies of these resources including mining district and field studies; develops computerized resource data bases, to answer state, federal, and industry requests for information; and encourages the prudent development of Utah's geologic resources. The **APPLIED GEOLOGY PROGRAM** responds to requests from local and state governmental entities for engineering-geologic investigations; and identifies, documents, and interprets Utah's geologic hazards. The **GEOLOGIC MAPPING PROGRAM** maps the bedrock and surficial geology of the state at a regional scale by county and at a more detailed scale by quadrangle. The **GEOLOGIC EXTENSION SERVICE** answers inquiries from the public and provides information about Utah's geology in a non-technical format. The **ENVIRONMENTAL SCIENCES PROGRAM** maintains and publishes records of Utah's fossil resources, provides paleontological and archeological recovery services to state and local governments, conducts studies of environmental change to aid resource management, and evaluates the quantity and quality of Utah's ground-water resources.

The UGS Library is open to the public and contains many reference works on Utah geology and many unpublished documents on aspects of Utah geology by UGS staff and others. The UGS has several computer data bases with information on mineral and energy resources, geologic hazards, stratigraphic sections, and bibliographic references. Most files may be viewed by using the UGS Library. The UGS also manages a sample library which contains core, cuttings, and soil samples from mineral and petroleum drill holes and engineering geology investigations. Samples may be viewed at the Sample Library or requested as a loan for outside study.

The UGS publishes the results of its investigations in the form of maps, reports, and compilations of data that are accessible to the public. For information on UGS publications, contact the Department of Natural Resources Bookstore, 1594 W. North Temple, Salt Lake City, Utah 84116, (801) 537-3320.

UGS Editorial Staff

J. Stringfellow	Editor
Vicky Clarke, Sharon Hamre	Graphic Artists
Patricia H. Speranza, James W. Parker, Lori Douglas	Cartographers

The Utah Department of Natural Resources receives federal aid and prohibits discrimination on the basis of race, color, sex, age, national origin, or disability. For information or complaints regarding discrimination, contact Executive Director, Utah Department of Natural Resources, 1594 West North Temple #3710, Box 145610, Salt Lake City, UT 84116-5610 or Equal Employment Opportunity Commission, 1801 L Street, NW, Washington DC 20507.



Printed on recycled paper

CONTENTS

ABSTRACT	1
INTRODUCTION	1
GEOTHERMAL RESOURCES	2
Geologic Setting	2
Heat-Flow and Electrical Surveys	4
Geohydrology	4
GEOTHERMAL DEVELOPMENT	4
MONITORING PROJECT	7
Temperature-Gradient Monitoring	7
Water-Level Measurements	7
Monitoring Results	7
NC-7	8
NC-9	8
NC-13	8
NC-15	8
NC-11	13
NUMERICAL ANALYSIS OF FLUID FLOW AND HEAT TRANSFER	13
Conceptual Model	13
Resource Analysis	15
Numerical Model	15
Model Geometry and Input Parameters	18
Finite-Element Grid	18
Boundary Conditions and Aquifer Recharge	18
Material Properties	18
Modeling Results	21
Conclusions	22
Recommendations	24
ACKNOWLEDGMENTS	24
REFERENCES	25
APPENDIX: Temperature-Gradient Data for Monitor Wells NC-7, NC-9, NC-11, NC-13, and NC-15	26

ILLUSTRATIONS

Figure 1. Geothermal areas and geographic features in southwestern Utah	2
Figure 2. Heat-flow map and well locations for the Newcastle geothermal area	3
Figure 3. Principal elements of the Newcastle geothermal system	5
Figure 4. Water levels in a well in NE $\frac{1}{4}$ SE $\frac{1}{4}$ NW $\frac{1}{4}$ section 18, T.36S., R.15E. of the Salt Lake Base Line	6
Figure 5. Water level changes in monitor wells NC-7, -9, and -11	8
Figure 6. Temperature-depth summary of Newcastle monitor well NC-7	9
Figure 7. Temperature-depth summary of Newcastle monitor well NC-9	10
Figure 8. Temperature-depth summary of Newcastle monitor well NC-13	11
Figure 9. Temperature-depth summary of Newcastle monitor well NC-15	12
Figure 10. Temperature-depth summary of Newcastle monitor well NC-11	14
Figure 11. Conceptual model for ground-water flow in the Newcastle geothermal system	15
Figure 12. Numerical modeling domain and boundary conditions for two-dimensional simulations of coupled fluid flow and heat transfer at Newcastle	16
Figure 13. Finite element mesh used in numerical simulations	17
Figure 14. Boundary conditions applied to solve the coupled fluid-flow and heat-transfer boundary value problem	19
Figure 15. Areas assigned material property values listed in table 1	20
Figure 16. Simulation results	22
Figure 17. Comparison of computed and observed thermal plumes	23

TABLE

Table 1. Parameter values used in final simulation	21
--	----

CONVERSION FACTORS

Note:

In the interest of clarity, SI units of measurement are generally used throughout this report. English equivalents are not listed in the text, but following is a list of useful conversions.

Length:

1 meter (m) = 3.281 feet (ft)
1 kilometer (km) = 0.6214 mile (mi)

Area:

1 m² = 10.76 ft²
1 km² = 0.3861 mi²
1 hectare (ha) = 10,000 m² = 2.47 acres

Volume:

1 liter (L) = 0.2642 gallon (gal)

Mass:

1 kilogram (kg) = 2.205 pounds (lb)

Flow rate:

1 liter per second (L/s) = 15.85 gallons per minute (gal/min)

Temperature:

degrees Celsius (°C) = 5/9 (degrees Fahrenheit [°F] - 32)
Kelvins (K) = °C + 273.15

Temperature gradient:

1°C/km = 0.05486°F/100 ft

Energy/Power:

1 joule (J) = 0.2390 calorie (cal)
1 J = 9.485x10⁻⁴ British thermal unit (Btu)
1 watt (W) = 1 J/s
1 milliwatt (mW) = 0.001 W
1 kilowatt (kW) = 1,000 W
1 megawatt (MW) = 1,000 kW = 3.154x10¹³ J/yr

Heat flow:

1 mW/m² = 2.390x10⁻⁸ cal/cm•s
1 mW/m² = 2.390x10⁻² heat-flow unit (HFU)

Thermal conductivity:

1 W/m•K = 2.390 mcal/cm•s•°C

Mention of brand or trade names does not imply endorsement by the Utah Geological Survey.

EFFECT OF GEOTHERMAL DRAWDOWN ON SUSTAINABLE DEVELOPMENT, NEWCASTLE GEOTHERMAL AREA, IRON COUNTY, UTAH

by
Robert E. Blackett¹, Howard P. Ross², and Craig B. Forster²

ABSTRACT

Discovered in 1975 by local farmers, the Newcastle geothermal resource has developed slowly. Pumping of geothermal water from the unconfined aquifer for space heating, mainly for commercial greenhouses, began in the early 1980s, and by 1988 three greenhouse complexes were producing tropical plants and vegetables for sale. One of the early operators went out of business, and in 1993 a California-based company purchased land, drilled new wells, and began construction of the first stage of a large-scale, geothermally heated greenhouse development.

Investigations by various organizations to characterize the geological and geophysical aspects of the system did not address the long-term, geohydrologic effects of large-scale withdrawal from the geothermal reservoir. Because future demands on the geothermal aquifer could stress the long-term productivity of the resource, we examined changes in the thermal regime of the system for the period 1976 through 1995.

We present results of detailed, periodic temperature-gradient monitoring of available monitor wells during the past three years and compare them to readings made in 1976 and 1988. Temperature-gradient measurements made in five monitor wells between 1993 and 1995 show significant temperature changes with time, although no effects on thermal water production were reported by the operators. All monitor wells show seasonal temperature fluctuations above the water table which correlate with seasonal air-temperature changes. Since 1976, monitor wells located along the northeast margin of the system (NC-7 and NC-9) exhibited temperature declines of 2 to 7°C below the water table. Since 1988, monitor well NC-13, located in the northeastern part of the system, showed temperature increases above 90 m and temperature decreases below 90 m. NC-15, also located in the northeastern part, showed small temperature fluctuations but has

had a general increase of about 4°C below the projected water table. The most significant temperature changes occur near the top of the thermal aquifer in monitor well NC-11, located adjacent to a producing well, where temperatures dropped by as much as 10°C over a 20-m interval between August 1993 and March 1995.

A two-dimensional, steady-state, numerical model developed by C.B. Forster roughly simulates the observed heat flow and suggests that current levels of geothermal production may affect the thermal regime. The impact of future, expanded production is, therefore, uncertain. The two-dimensional, steady-state simulator is strongly influenced by aquifer thickness, permeability, and thickness of the overlying unsaturated zone - parameters for which the spatial variability is not adequately known. Therefore, a long-term program to gather data using new, strategically placed monitor wells, and development of a two-dimensional transient simulator are recommended. The two-dimensional transient simulator, using data gathered from a program of testing in new monitor wells, would provide insight into the interference between wells and help determine the long-term effects to the overall geothermal system.

INTRODUCTION

Newcastle, a rural farming community, is located 48 km west of Cedar City, Utah (figure 1). Since the discovery of geothermal water in 1975, various geothermal developers and government agencies have been interested in the Newcastle area. These groups drilled exploratory wells and temperature-gradient monitor wells, and used various geophysical methods to study the geothermal system. U.S. Department of Energy-sponsored studies by the University of Utah (Chapman and others, 1981; Clement,

¹Utah Geological Survey, Department of Natural Resources, Salt Lake City, Utah

²Energy and Geoscience Institute, Department of Civil and Environmental Engineering, University of Utah.

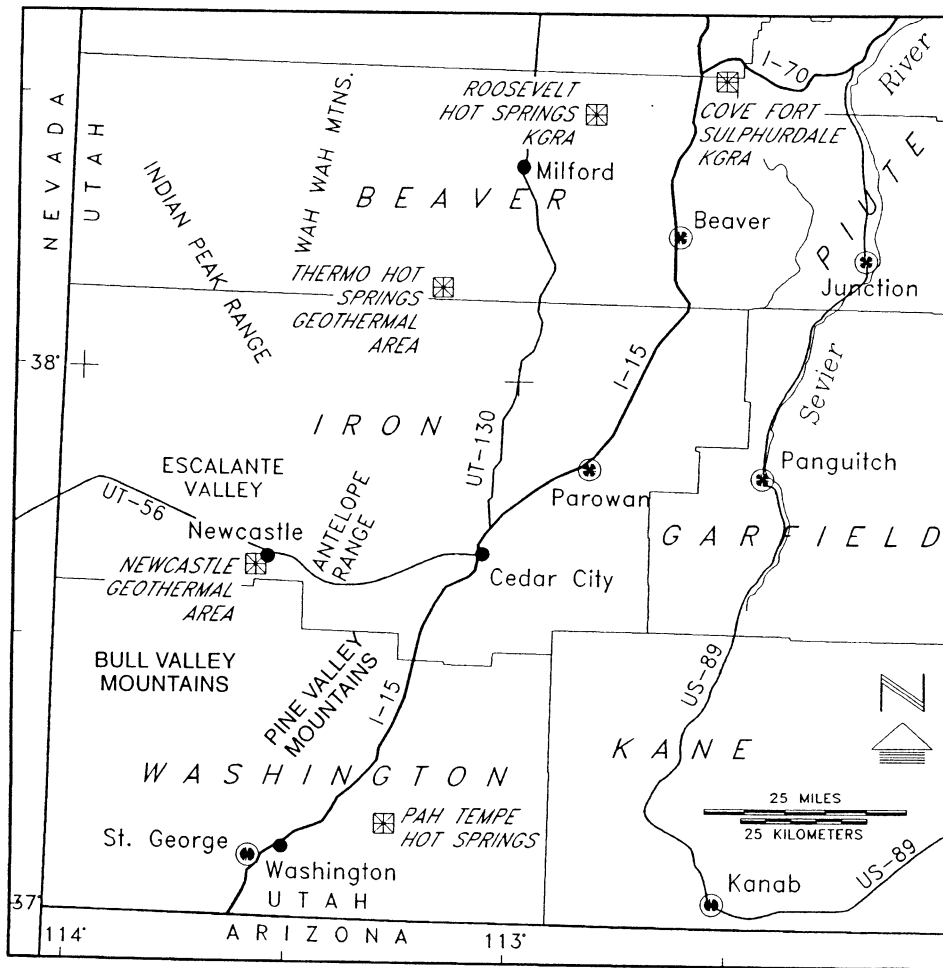


Figure 1. Geothermal areas and geographic features in southwestern Utah.

two 155-meter production wells at rates up to 100 L/s, through heat exchangers, and eventually to an injection well. The exit water is injected at 60°C into the unconfined aquifer about 610 m down gradient from the production well. No major changes in water temperatures or water levels have been reported by the operators, but increased fluid production could eventually stress the aquifer and result in temperature or volumetric declines in production wells.

The greenhouse businesses at Newcastle provide an expanded tax base and desirable, year-round employment well suited to this rural area. We need to greatly improve our understanding of the hydrothermal system and plan for sustainable long-term development which will provide continued employment and protect the capital invested in these facilities. This report describes preliminary monitoring efforts, discusses issues which could surface during future development, and outlines a proposed, expanded monitoring program.

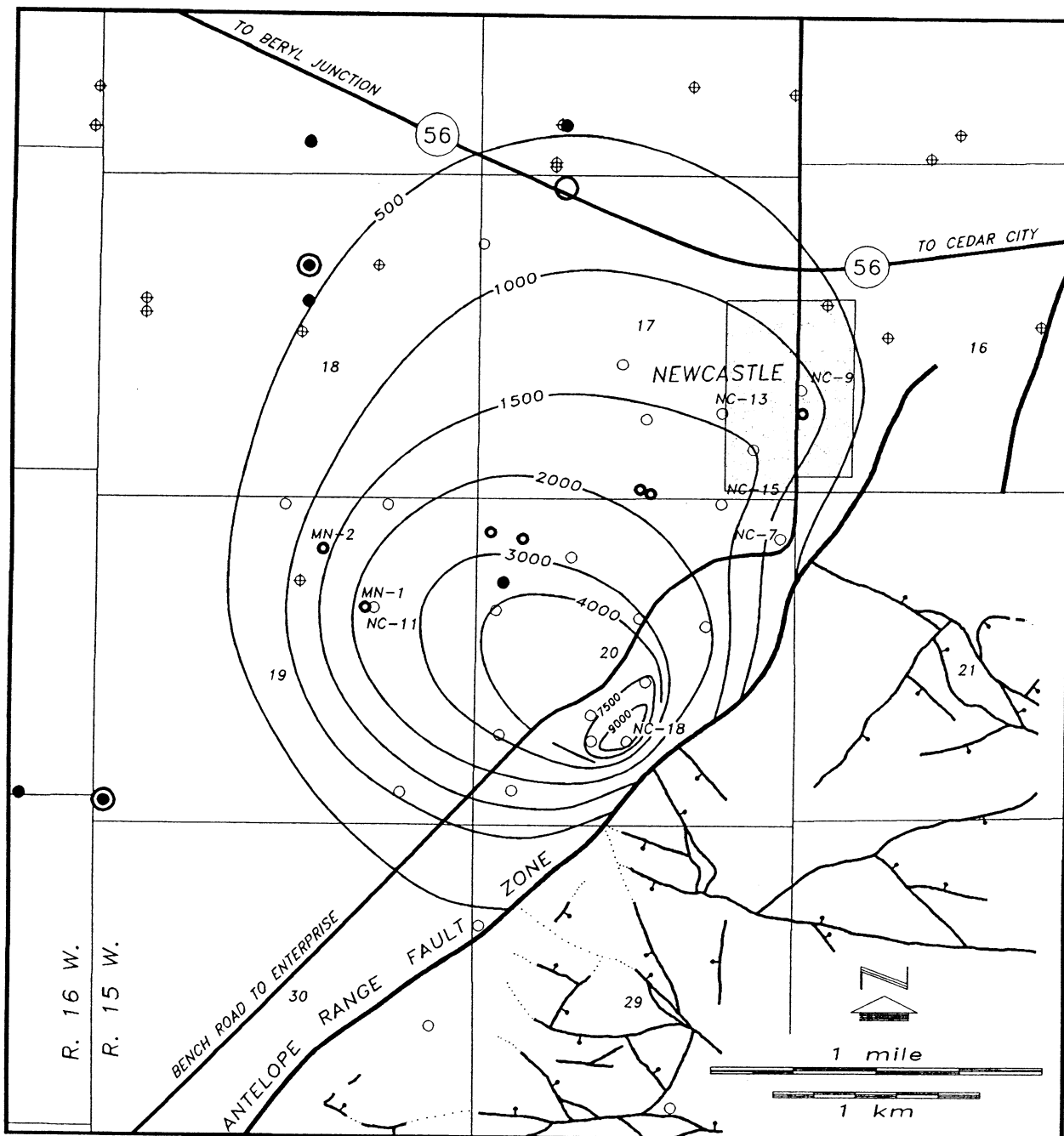
1981), the U.S. Geological Survey (USGS) (Rush, 1977, 1983), the Utah Geological Survey (Blackett and others, 1990; Blackett and Shubat, 1992), and the University of Utah Research Institute (Ross and others, 1990, 1991) defined a covered up-flow zone along the nearby Antelope Range fault. From this up-flow zone, geothermal water moves into a shallow (50-70 m), unconfined alluvial aquifer that allows the thermo-chemical outflow plume of the hydrothermal system to spread to the west and north beneath the Escalante Valley (figure 2). Commercial greenhouse operators tap this outflow plume by production wells 155 meters deep and use the hot water for space heating.

By 1988, three commercial greenhouses and a chapel of the Church of Jesus Christ of Latter-day Saints were using thermal fluids for space heating, disposing of the cooled fluid mainly in percolation pits and drain fields. Beginning in 1993, Milgro Nurseries purchased property, drilled production and injection wells, and constructed three greenhouses enclosing 4.9 hectares (ha). Thermal water at a well-head temperature of 89°C is pumped from

GEOHERMAL RESOURCES

Geologic Setting

The Newcastle area is located at the southeastern margin of the Escalante Valley (figure 1), an elliptical basin measuring roughly 70 by 45 km on the margin of the Basin and Range-Colorado Plateau transition zone. It is surrounded by mountains and hills composed primarily of Tertiary ash-flow tuff ranging from 32 to 19 million years old, and rhyolite and dacite flows and domes ranging from 13 to 8.5 million years old. The Antelope Range fault marks the southeastern margin of the Escalante Valley (figure 2). Geological and geophysical studies indicate that at Newcastle thermal fluids rise beneath alluvial cover at the intersection of a northwest-oriented fault and fracture zone and the northeast-oriented Antelope Range fault (Ross and others, 1990; Siders and others, 1990; Blackett and Shubat, 1992).



E X P L A N A T I O N

- | | | | |
|---|---|---|--|
| ● | USGS water-chemistry monitor well | ● | geothermal production well |
| ○ | USGS water-level monitor well | ○ | thermal-gradient drill hole |
| ⊙ | USGS water chemistry and water-level monitor well | — | heat-flow contour (values in mW/m ²) |
| ⊕ | water well | — | bedrock fault, bar and ball on down-thrown side |

Figure 2. Heat-flow map and well locations for the Newcastle geothermal area showing designations for production wells and monitor wells, principal faults, and heat-flow contours.

Bedrock units exposed in the hills southeast of Newcastle, described in detail by Siders and others (1990), range in age from late Cretaceous to late Miocene. They consist of upper Cretaceous and lower Tertiary sedimentary units overlain by a series of regional, mid-Tertiary ash-flow tuff and volcanoclastic rocks capped by local rhyolite and dacite flows. Various unconsolidated to semi-consolidated deposits lie stratigraphically above the bedrock units and constitute much of the Escalante Desert valley fill. These units include upper Miocene to Pliocene coarse fluvial sediments deposited around the margin of the Escalante Valley, Pliocene to lower Pleistocene piedmont-slope alluvium, and Pleistocene to Holocene distal fan deposits (Siders and others, 1990).

The alluvial units of the Escalante Valley generally terminate at the Antelope Range fault. This structure is a major north-northeast-trending, range-bounding normal fault that defines the southeastern side of the Newcastle graben, a feature first suggested by the regional gravity work of Pe and Cook (1980). Detailed gravity surveys, reported by Blackett and Shubat (1992), suggest that valley-fill deposits within the Newcastle graben may be 1.6 km thick. Anderson and Christenson (1989) suggest a middle- to late-Pleistocene age for the most-recent surface-rupturing event along the Antelope Range fault. Geologic mapping of bedrock units southeast of Newcastle revealed that the greatest bedrock offset (600 to 900 m) occurs along northwest-striking faults (Shubat and Siders, 1988; Blackett and Shubat, 1992). Several of these faults project beneath the valley fill and onto the footwall of the Antelope Range fault near the center of the mapped thermal anomaly (figure 2).

Heat-Flow and Electrical Surveys

Assuming a background heat flux of 100 milliwatts per square meter (mW/m^2), Blackett and Shubat (1992) reported an anomalous heat loss of 12.4 megawatts (MW). A more recent calculation, reported by Ross and others (1994), which accounted for corrected well positions and used the method of D.S. Chapman (in Blackett and others, 1990), yielded an anomalous heat loss of 13.8 MW.

Ross and others (1990) completed electrical resistivity and self-potential (SP) studies which provided independent evidence for the location of the thermal fluid up-flow zone. A well-defined 108 millivolt (mV) SP minimum was mapped between temperature-gradient monitor wells with greatest heat flow (NC-5,-14,-18,-19) and above the projected intersection of northwest-trending structures with the Antelope Range fault. Two lesser minima of -44 mV and -36 mV were also mapped to the southwest, above the buried Antelope Range fault. Numerical models of dipole-dipole resistivity profiles resolve

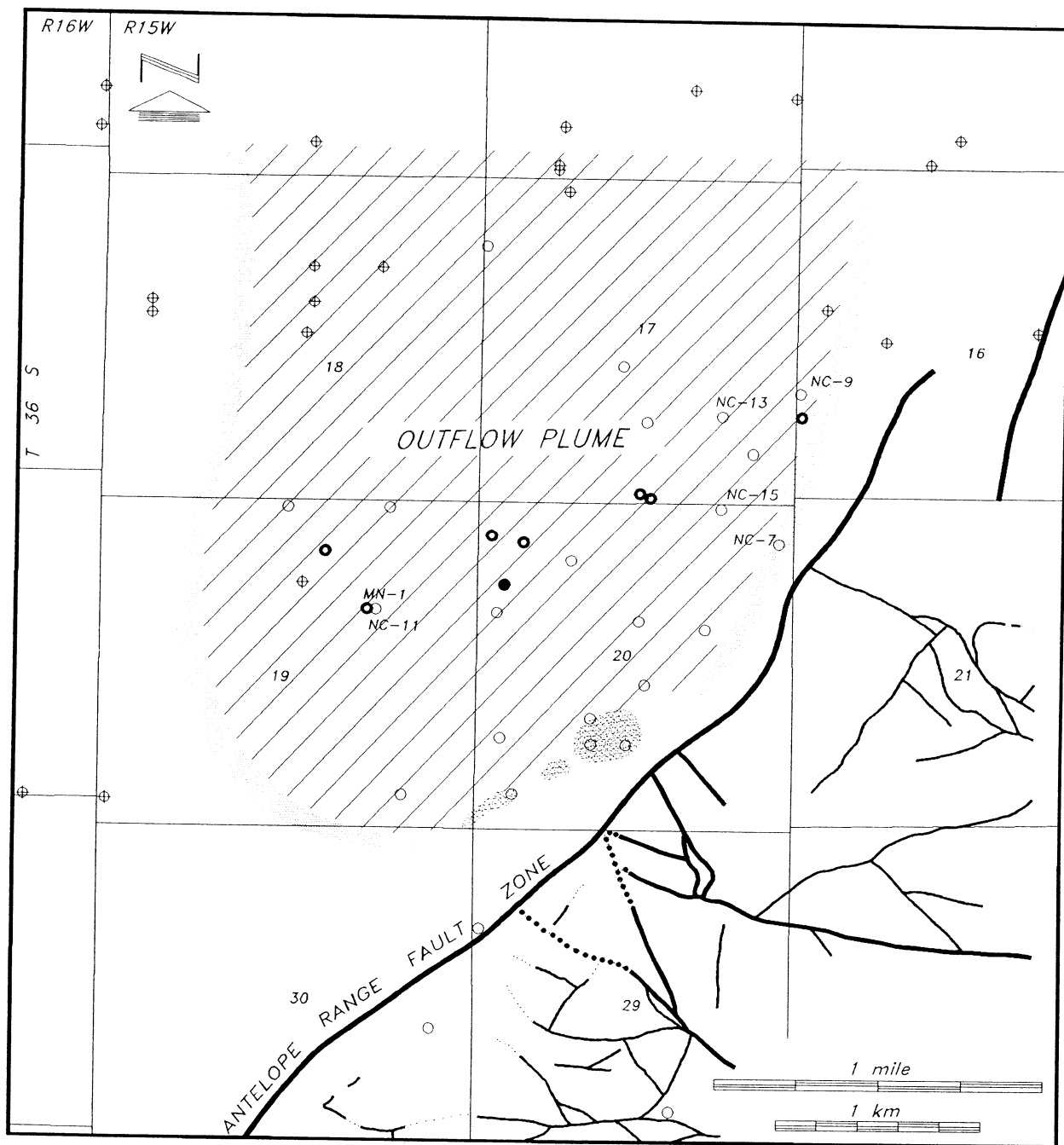
near-vertical low-resistivity (4 ohm-m) bodies which are interpreted as up-flow zones. A low-resistivity (4 ohm-m) layer at a depth of about 45 m within the alluvium extending to the northwest is interpreted as the geothermal outflow plume. Figure 3 summarizes interpreted self-potential, resistivity, and heat-flow data for the Newcastle geothermal system.

Geohydrology

Ground water is present mainly within the unconsolidated and semiconsolidated valley-fill units of the Escalante Valley. The principal aquifer, described by Mower (1981), is tapped by numerous irrigation wells throughout the valley. Wells pump such large volumes of water for irrigation that ground water no longer follows the natural flow path northeastward, but rather, flows to an artificial water-table depression near Beryl Junction. Near Newcastle, the potentiometric surface is slightly elevated (3 m) with respect to the Beryl-Enterprise area; we believe this is due to the geothermal system discharging into the principal aquifer. The geothermal discharge originates in the shallow subsurface near the intersection of the range-bounding Antelope Range fault and high-angle bedrock faults (figure 2). Thermal fluid spills from this discharge, or up-flow zone, into the principal aquifer of the Escalante Valley, and moves as a thermal-chemical outflow plume northwestward down the hydrologic gradient. The effect of irrigation withdrawal from the Escalante Valley aquifer on the geothermal system at Newcastle is unclear. Ground-water levels in the Escalante Valley near Newcastle have declined over the past 20 to 30 years mainly due to withdrawals for irrigation of croplands in the valley. Between 1975 and 1994, the static water level in a well located in the north-central part of section 18, T. 36 S., R. 15 W., of the Salt Lake Base Line (figures 2 and 4) declined by about 12 m (USGS Water Resources Division, Cedar City office, unpublished data). Since the geothermal system and the ground-water reservoir combine in the outflow zone, ground-water declines could conceivably affect the geothermal system.

GEOTHERMAL DEVELOPMENT

In the late 1970s and early 1980s, developers drilled several geothermal supply wells to provide heat for a new greenhouse industry. Troy Hygro Systems, Hildebrand Greenhouses, and Anzalone Greenhouses (later acquired by Utah Natural Growers) all developed water-supply wells in the thermal aquifer and disposed of spent fluids in shallow percolation pits, drain fields, or injection wells.



E X P L A N A T I O N

- Geothermal supply well
- Thermal-gradient drill hole
- ⊕ Water well
- Major bedrock fault
- - - Minor bedrock fault
- ▨ Inferred hydrologic barrier
- ▤ Geothermal up-flow zone with possible high-temperature reservoir at depth

Figure 3. Principal elements of the Newcastle geothermal system from geological and geophysical data (after Ross and others, 1990).

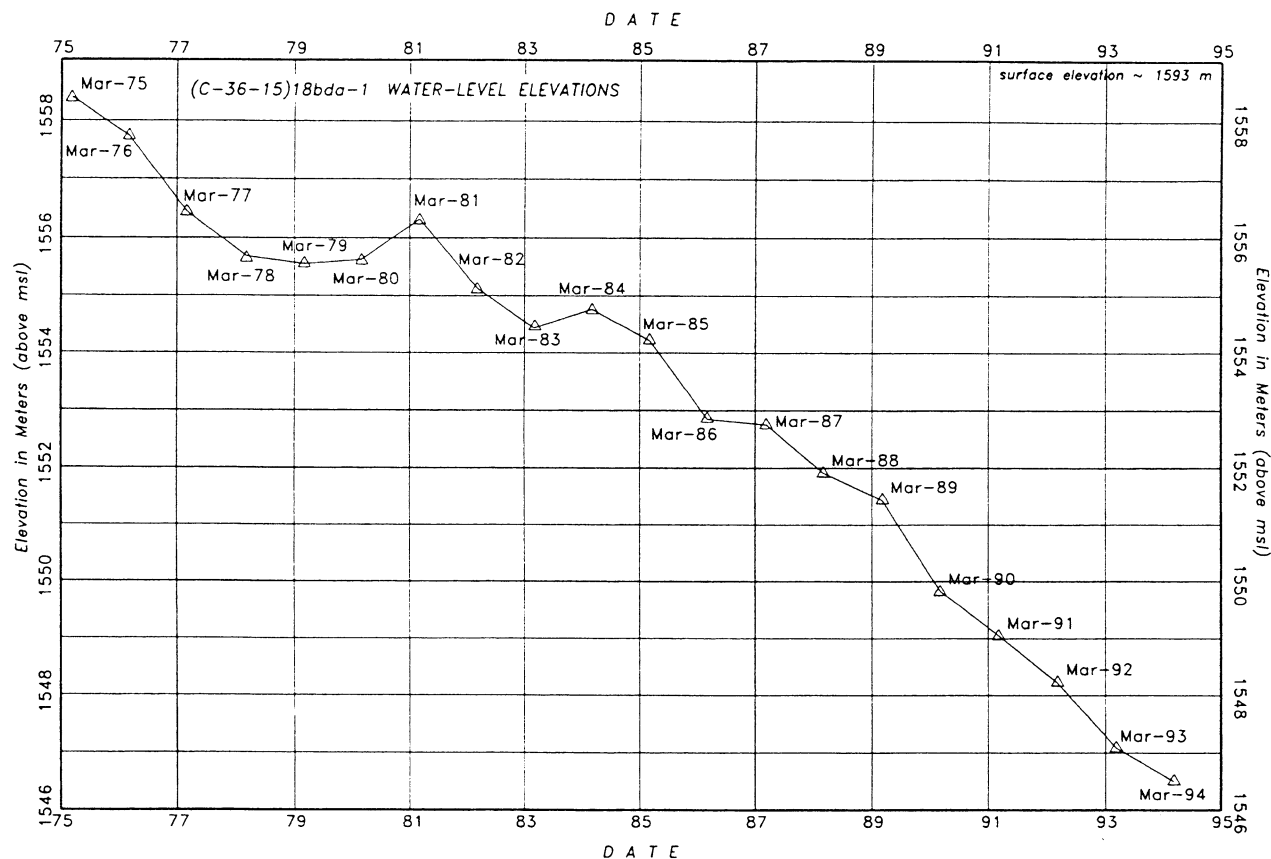


Figure 4. Water levels in a well located in the NE $\frac{1}{4}$ SE $\frac{1}{4}$ NW $\frac{1}{4}$ Section 18, T. 36 S., R. 15 E. After data from U.S. Geological Survey Water Resources Division, Cedar City office.

The greenhouses of Troy Hygro Systems, inactive since 1990, were recently refurbished and are now operated by the Christensen family of Newcastle. In addition to the greenhouses, a Mormon chapel in Newcastle began using geothermal water pumped from a 140-m well and through a surface heat exchanger (Hal Gardner, Church of Jesus Christ of Latter-day Saints, verbal communication, 1994). Some Newcastle residents also drilled wells and equipped them with crude down-hole heat exchangers for space heating, but after completion of the Kern River natural gas pipeline through Newcastle in 1993, low-cost natural gas was readily available, thereby lessening the attractiveness of geothermal water for residential space heating.

In July 1993, Milgro Nurseries, Inc. began developing a state-of-the-art greenhouse facility with construction of a 1.62-ha greenhouse, and drilling of a 155-m production well (MN-1). MN-1, drilled 19 meters west of temperature-gradient monitor well NC-11, produces up to 76 liters (L) per minute of geothermal water at a temperature of about 89°C. The geothermal water circulates from the production well, through a heat exchanger, to an injection well down gradient from the production well. At the injection well, the water has cooled to about 60°C.

The production well performed without problems throughout the winter of 1993-94 with no noticeable decline in temperature or water level. Beginning in the spring of 1994 and continuing through summer, Milgro reported a drop in production temperature of about 6°C. Milgro also reported this same condition during the spring and summer of 1995 and 1996. In late 1994, decline in injectivity dictated that Milgro dispose of spent fluid into temporary percolation pits. In early 1996, Milgro installed a dedicated pump in the injection well for periodic back flushing. Since back flushing began, Milgro has experienced no underground injection problems (William Gordon, Milgro Nurseries, Inc., verbal communication, 1996). In March 1996, Milgro drilled a second production well (MN-2) and completed construction of a third greenhouse, bringing the total area covered to 4.9 ha.

Additional development of the thermal aquifer, and perhaps the source zone of the geothermal system, might take place since potential developers have expressed interest in the Newcastle geothermal area. Milgro Nurseries has expressed plans for a systematic expansion of up to seven greenhouses (11 ha total) if market conditions permit. Milgro has also shown interest in expanding into other

agricultural products and aquaculture if they could be assured of an adequate supply of geothermal water. In addition to greenhouse development, the up-flow zone, with temperatures above 130°C, may be suitable for development of power generation using binary technology. Besides residential service, local electrical demands include pumping for irrigation to support a considerable agricultural industry (spring through early fall) and pumping of thermal water to support the greenhouse industry (fall through spring).

MONITORING PROJECT

Temperature-Gradient Monitoring

Reservoir testing of the thermal aquifer has been very limited, and the long-term production potential is not known. Anticipating possible large, long-term withdrawals of fluid from the thermal aquifer, the Utah Geological Survey (UGS) and the University of Utah Research Institute (UURI; now part of the Energy and Geoscience Institute, University of Utah) began a program of temperature monitoring in August 1993.

The monitoring consisted of periodic, detailed temperature-depth measurements in five temperature-gradient monitor wells usually at one- to three-month intervals. The first set of these temperature profiles made in August 1993 are regarded as the baseline because a minimum of thermal fluids were being pumped for space heating, and because initial testing of Milgro well MN-1 was finished. Temperature logs were completed in NC-7, -9, -11, and -15 on 31 August 1993 and monitor well NC-13 was added to the monitoring network on 5 October 1993. Temperature gradients for all of these monitor wells were reported in earlier studies by Rush (1977), Clement (1981), and Blackett and others (1990).

Interim technical reports (Blackett, 1993, 1994) document: (1) baseline temperatures, (2) previous and current-month temperatures, and (3) incremental and cumulative temperature changes. The appendix contains a summary of these data. Temperatures were measured usually at 20-m intervals above the water level (readings made in air) and at 2-m intervals below the water level. Temperature-gradient monitor wells are completed by installing sealed, slim-diameter casing; backfilling the annulus with cuttings, soil, or cement; and finally filling the casing with water. This prevents communication of water in the casing with ground water and allows accurate temperature-gradient measurements. Since water levels in monitor-wells NC-7, NC-9, and NC-11 appear to fluctuate seasonally, we suspect that the casing strings in these monitor wells may be ruptured within the saturated zone.

Although the distribution (figure 2), depth, and com-

pletion of the monitor wells were not ideal, we felt that periodic temperature measurements could provide indications of changes in the thermal aquifer in response to natural cycles and/or geothermal production. Monitor well NC-7 is located near the Antelope Range fault about 1,100 meters north of the up-flow zone, and NC-9 is near the church supply well. Monitor wells NC-13 and NC-15 are within 610 m of the Hildebrand Greenhouse wells, and NC-11 is only 19 m east of Milgro Nurseries' supply well (MN-1).

Temperature measurements were made with an NP Instruments brand, high-precision, thermistor probe and temperature logging equipment. Instrument characteristics and monthly calibrations result in a temperature measurement precision of 0.01°C, but convection within the well can reduce measurement accuracy to $\pm 0.05^\circ\text{C}$.

Water-Level Measurements

Depths to water levels were made in three of the monitor wells using a Soiltest Water Level Indicator. Monitor wells NC-7, -9, and -11 were initially completed with a sealed casing and filled with water to permit accurate temperature-depth measurements, but the casing strings in these three monitor wells have apparently ruptured within the saturated zone; therefore, water levels may approximate the position of the water table. The casing strings in NC-13 and NC-15 were installed as closed-loop heat exchangers and do not provide insight into the ground-water levels. Water levels in the three monitor wells measured from November 1993 through May 1994 are summarized in figure 5. Readings from NC-7 show a systematic rise of 0.8 meter in water level from November to April, while water level in NC-9 rose by 2.4 meters over this same period. Water level in NC-11 declined 0.2 meter during the winter, but by April had recovered to the November level. Even though the greenhouses use more geothermal fluid during the winter, the water table rises. We feel this increase in water level during the winter is more likely a response of the aquifer to reduced pumping for irrigation elsewhere in the Escalante Valley rather than to increased recharge. Water levels in all three monitor wells declined between April and May, probably in response to renewed ground-water withdrawals for irrigation.

Monitoring Results

Figures 6 through 10 summarize baseline temperatures and observed temperatures in the monitor wells for selected months, from August 1988 to October 1996. Sev-

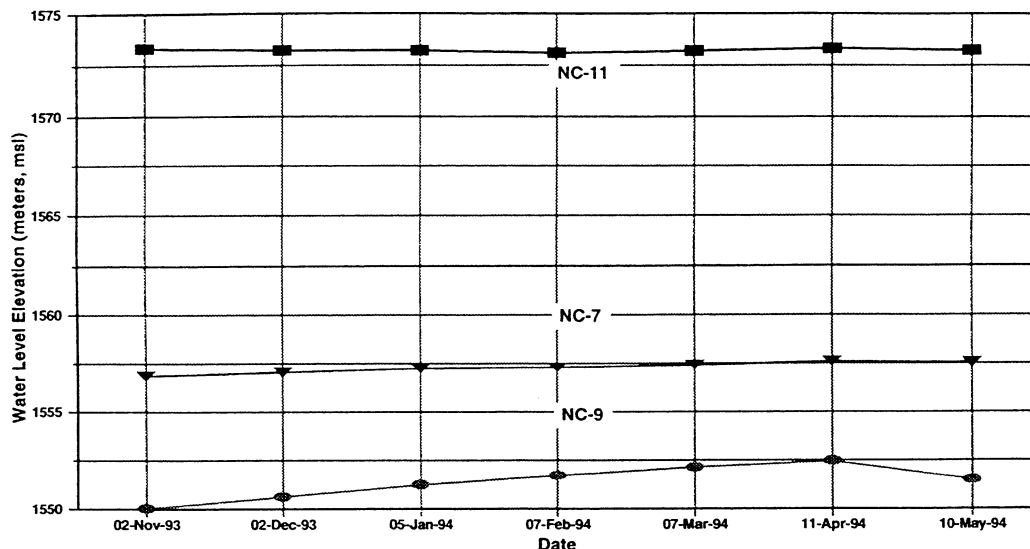


Figure 5. Water level changes in monitor wells NC-7, NC-9, and NC-11 from November 1993 through May 1994. Well locations are shown in figure 2.

eral factors may contribute to temperature changes measured in Newcastle monitor wells. Climatic and seasonal air temperature variations may perturb shallow temperatures above the water table. Reduced pumping for irrigation (fall and winter) in the main part of the Escalante Valley may result in increased inflow of cool, shallow ground water and water-table rises. Short-term production of thermal fluids may increase temperatures in more permeable zones of the thermal aquifer, as hotter water moves from the source zone toward the pumped wells. Less permeable zones may show little change on a seasonal or short-term basis.

NC-7

This well was drilled to about 90 m depth and penetrated only the upper part of the thermal aquifer. Temperatures were significantly cooler (0° - 0.5°C) above the water table through the winter months, and slightly warmer (0.02° - 0.06°C) near the bottom (80-91 m) of the well (figure 6). Bottom-hole temperatures approached baseline values ($+0.01^{\circ}\text{C}$) in March. Temperature profiles made in this well in 1976 (Rush, 1977; Clement, 1981) and 1988 (Blackett and others, 1990) indicate a general cooling within the aquifer of 2 - 3°C over the last 15 years.

NC-9

Temperatures in NC-9 became cooler overall during the monitoring period (figure 7). Drilled to about 90 meters depth, NC-9 penetrated only the upper part of the thermal aquifer. Comparing our readings with a temperature profile recorded by Rush (1977) indicates borehole cooling by as much as 10°C during the last 17 years.

NC-13

This monitor well, drilled to a depth of 121 m, contains two concentric pipes installed as a simple down-hole heat exchanger for space-heating of a residence. The heating system was never completed. Water level inside the inner casing is constant at about 5 m depth. A broad zone near the projected water table (60-80 meters depth) became progressively warmer (2 - 3°C). Minor warming that we observed through winter near the bottom of the well (100-120 m depth) reversed by March but remained slightly cooler than baseline values. A temperature profile of this well made in 1988 (Blackett and others, 1990) shows temperature increasing by as much as 10°C above 90 m and decreasing slightly below 90 m (figure 8).

NC-15

Monitor well NC-15 was drilled to 101 meters and completed with a simple U-shaped casing as a down-hole heat exchanger. Reportedly, the casing was filled with ethylene glycol (George Beacham, well owner, verbal communication, 1990) to be used as a working fluid, but the heating system was never completed. Overall, the borehole showed temperature fluctuations from 0.1° to 4°C , with the largest changes between about 56 and 63 m depth (figure 9). A temperature profile made in 1988 (Blackett and others, 1990) shows an overall increase in temperature of as many as five degrees over a six-year period. The temperature-depth profile has two distinct step-like features near 63 m and 86 m that could possibly be due to the type of well completion, or due to lithologic variations in the valley fill. The borehole does not completely penetrate the thermal aquifer.

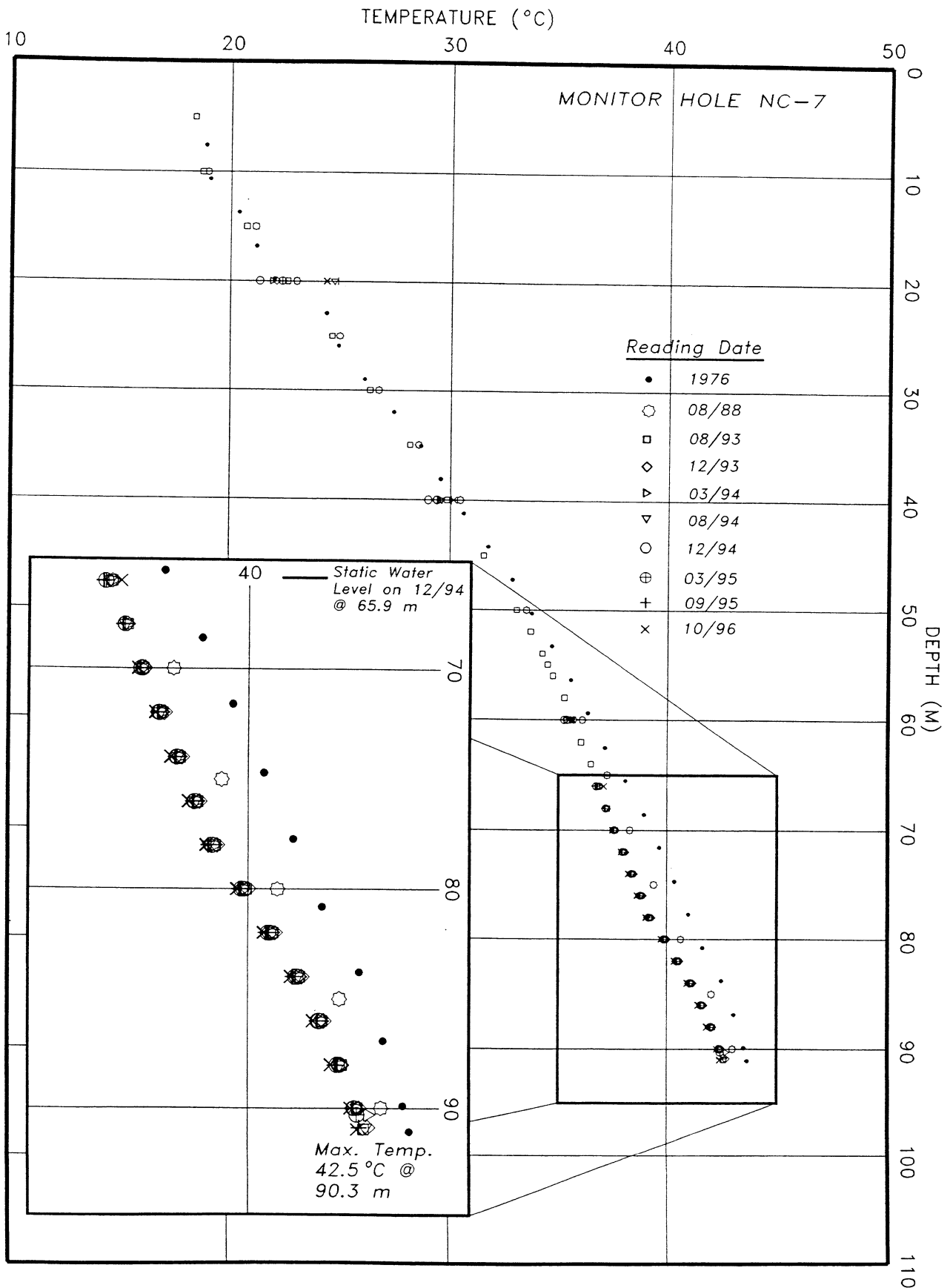


Figure 6. Temperature-depth summary for Newcastle monitor well NC-7. Plot illustrates the thermal profile based on 10 separate readings between 1976 (exact date unknown) and October 1996. Well location is shown in figure 2.

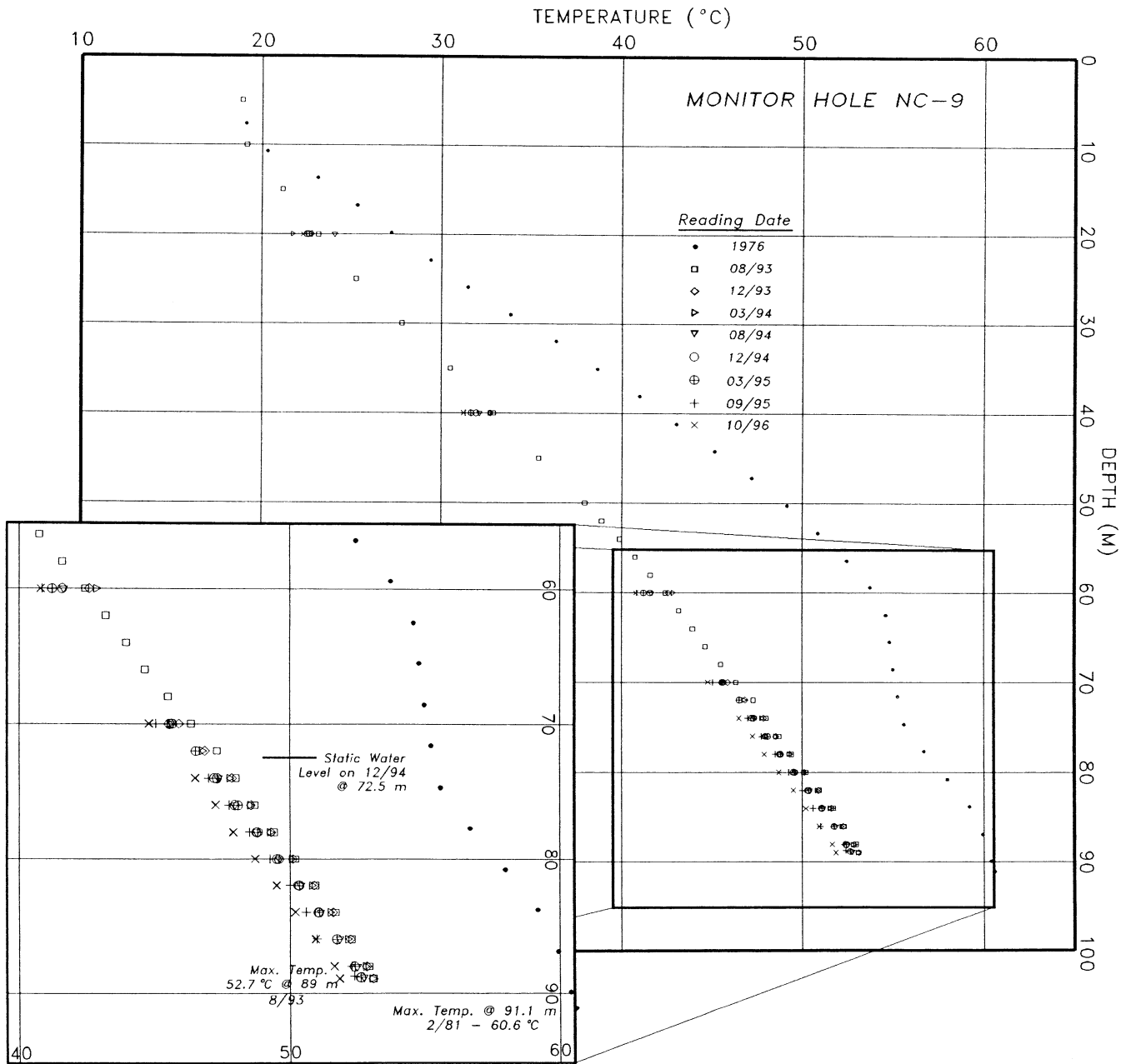


Figure 7. Temperature-depth summary for Newcastle monitor well NC-9. Plot illustrates the thermal profile based on nine separate readings between 1976 (exact date unknown) and October 1996. Well location is shown in figure 2.

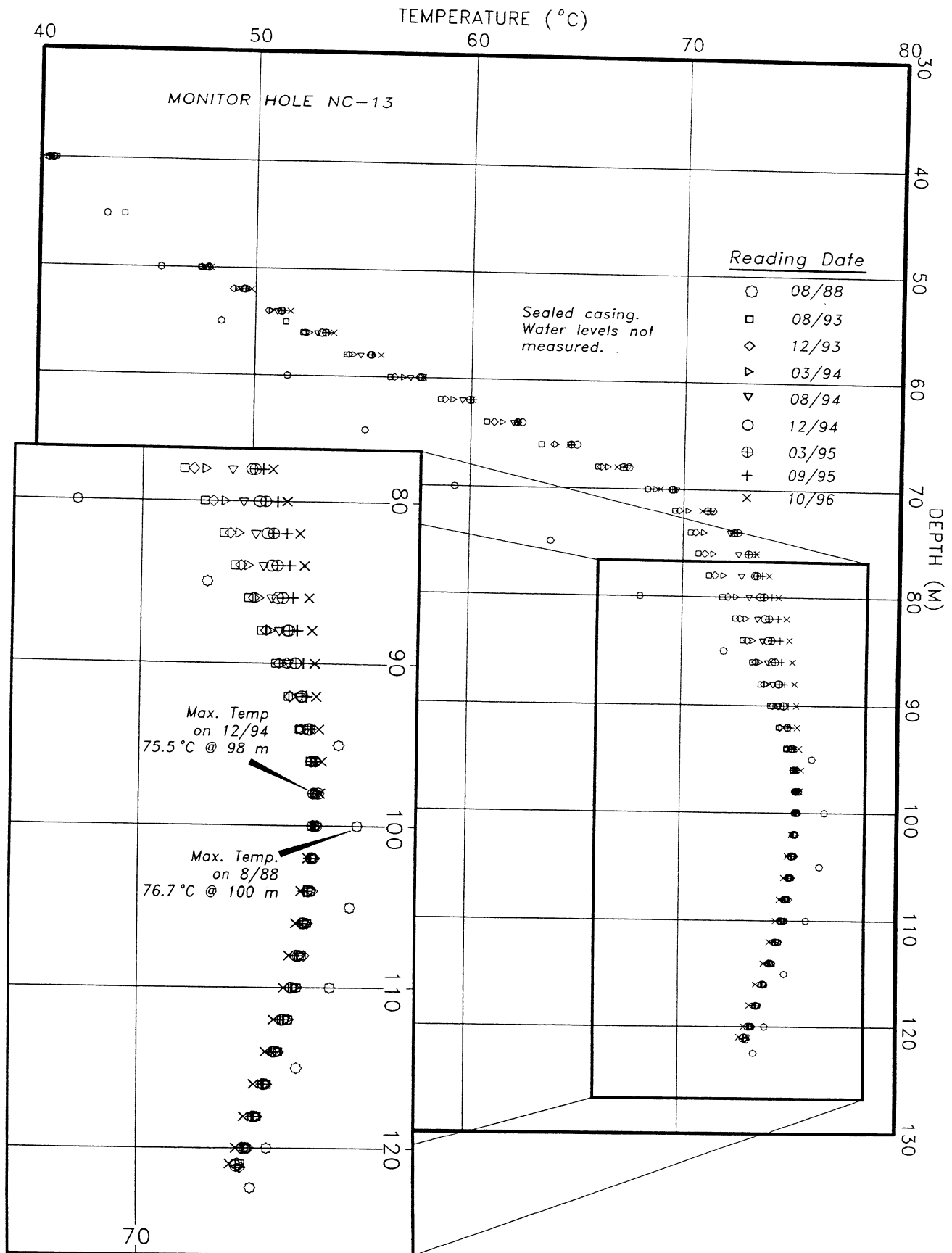


Figure 8. Temperature-depth summary for Newcastle monitor well NC-13. Plot illustrates the thermal profile based on nine separate readings between August 1988 and October 1996. Well location is shown in figure 2.

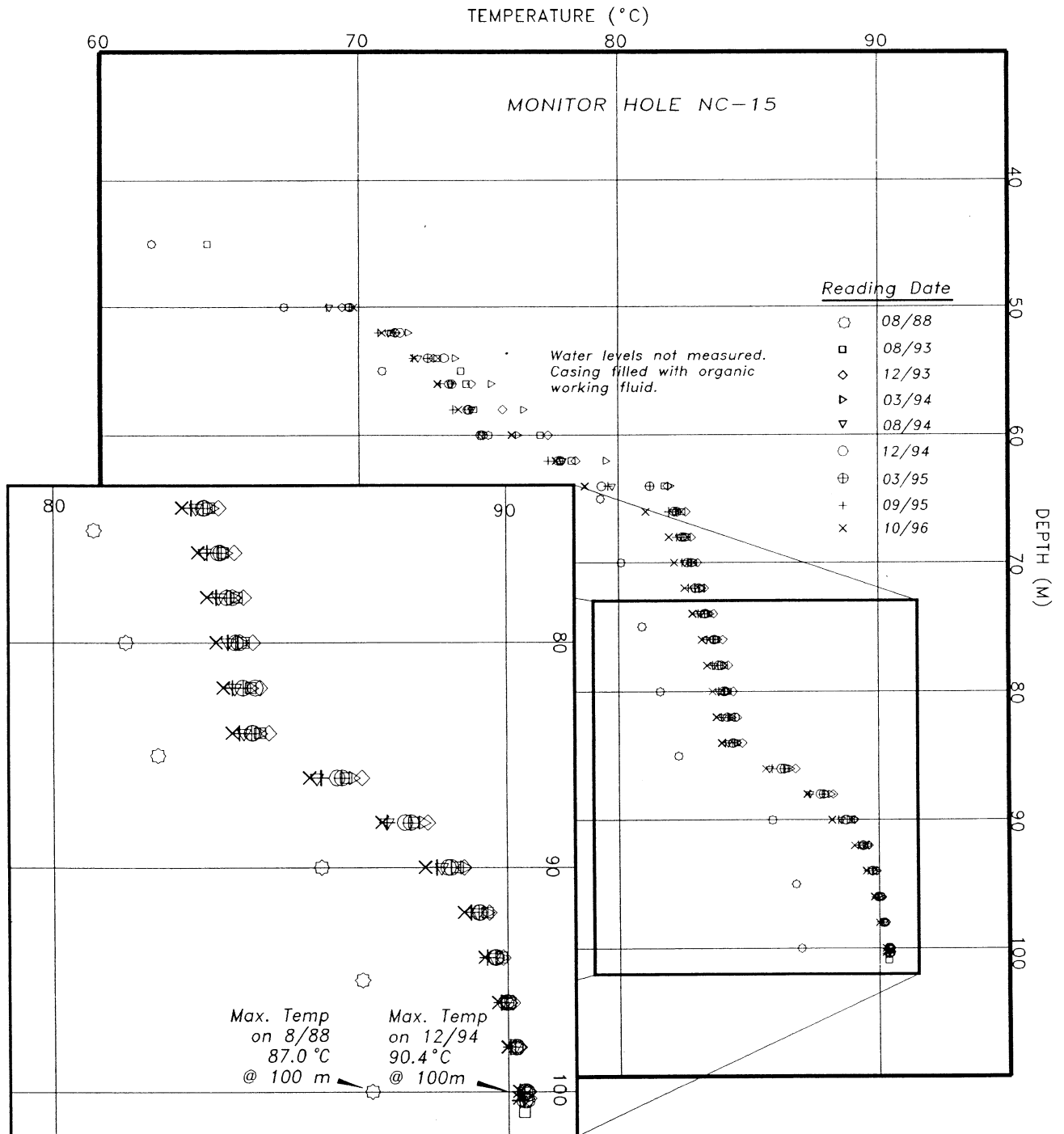


Figure 9. Temperature-depth summary for Newcastle monitor well NC-15. Plot illustrates the thermal profile based on nine separate readings between August 1988 and October 1996. Well location is shown in figure 2.

NC-11

This monitor well, located only 19 m eastward from the MN-1 production well, showed the most pronounced changes of all the monitor wells (figure 10). Temperatures above the water level declined by as much as 7°C, then recovered as heating demand declined. Temperatures within a 20-m zone below the water level declined from 6 to 9°C for the period between August 1993 and August 1994, recovered by about 4°C in December 1994, then declined again by March 1995. We interpret this as drawdown in a permeable zone near the top of the thermal aquifer in response to fluid production, with inflow of cooler water from the margins of the system. Generally, the part of the thermal aquifer below the 20-m near-surface zone warmed (90-130 m depth, 0.5° - 1.2°C). A zone near 125 m depth became slightly cooler and the bottom of the well (140-154.8 m depth) warmed slightly (0.1° to 0.2°C), possibly indicating permeability contrasts. Comparing temperature profiles measured in NC-11 in 1976 (Rush, 1977) and in 1988 (Blackett and others, 1990) with the more recent profiles shows a general temperature increase throughout the borehole (figure 10). The hottest part of the thermal zone has warmed about 5°C since 1976.

NUMERICAL ANALYSIS OF FLUID FLOW AND HEAT TRANSFER

Geothermal resource assessment requires understanding the interplay between the natural supply of heated water to a geothermal system and the impact of reservoir production. Important insight into the resource potential of the Newcastle geothermal system can be gained through numerical modeling of coupled fluid and heat transfer. By attempting to mimic the observed thermal regime with a numerical model, we can better understand how the system operates. If the model can be calibrated against observed data then we can also evaluate how production of hot water for geothermal heating might influence resource-management strategies.

Conceptual and numerical models of the Newcastle geothermal system are required to assist in planning for additional development with minimal adverse impact on existing users. Although a reasonable conceptual model has been formulated (Blackett and others, 1990), only preliminary modeling studies were performed prior to this study. Using a new simulator we can assess the validity of the conceptual model and provide an improved basis for resource assessment.

Conceptual Model

Blackett and others (1990) proposed the conceptual model for the Newcastle geothermal system shown in figure 11. Inferred patterns of flow are indicated by the apparent direction of fluid flow shown within the system. According to the model, meteoric water recharging in the Pine Valley Mountains-Antelope Range highlands circulates deeply within bedrock units before discharging to the valley-fill sediments. In the absence of the more permeable fault zones shown in figure 11, insufficient heat would be extracted to form a concentrated geothermal resource. Thus, the enhanced permeability associated with the intersection of two major faults provides for a well-defined conduit structure that focuses the up-flowing thermal fluid. The locations and sizes of the up-flow zones and thermal plumes inferred from SP and resistivity surveys are shown in figure 3. Clement (1981) and Rush (1983) estimate that a minimum discharge of approximately 0.032 cubic meters per second (32 liters per second) from these up-flow zones is required to produce the estimated heat loss of 13 MW. Ross and others (1994) subsequently updated this estimate to 13.8 MW. The conceptual models of Clement (1981) and Chapman and others (1981) differ from the one shown in figure 11 because they assumed a localized high-temperature fluid source injected into a static ground-water flow system. In our model, however, we assume that the hot water discharges into the shallow ground-water flow system that circulates within the valley-fill sediments.

Ground water with elevated temperature and relatively high total dissolved solids (TDS) discharging from the fault zone intersection must mix with cool and relatively fresh ground water circulating in the valley-fill deposits. This mixing process may cause siliceous and/or carbonate minerals to precipitate within the porous sediments that, in turn, may cause reduced permeability in the vicinity of the mixing zone. In the early stages of system evolution the region of fluid mixing was likely located at the base of the valley-fill sediments. Through time, however, the mixing of fluids in the sediments may have contributed to progressive construction of a low-permeability seal that extends upward from the original point of discharge at the bedrock surface to a position relatively close to the ground surface (figure 11). Concurrent downward movement of the hanging-wall block of the mountain-bounding fault likely contributes to upward growth of the precipitate seal. Development of the seal may be enhanced wherever boiling occurs at the water table (for example, in the vicinity of NC-18; shown in figures 2 and 11).

Heated ground water discharging to the valley-fill deposits forms a thermal plume (figure 2) with a size and shape controlled, in large part, by the character of the shallow ground-water flow system. A chemical plume,

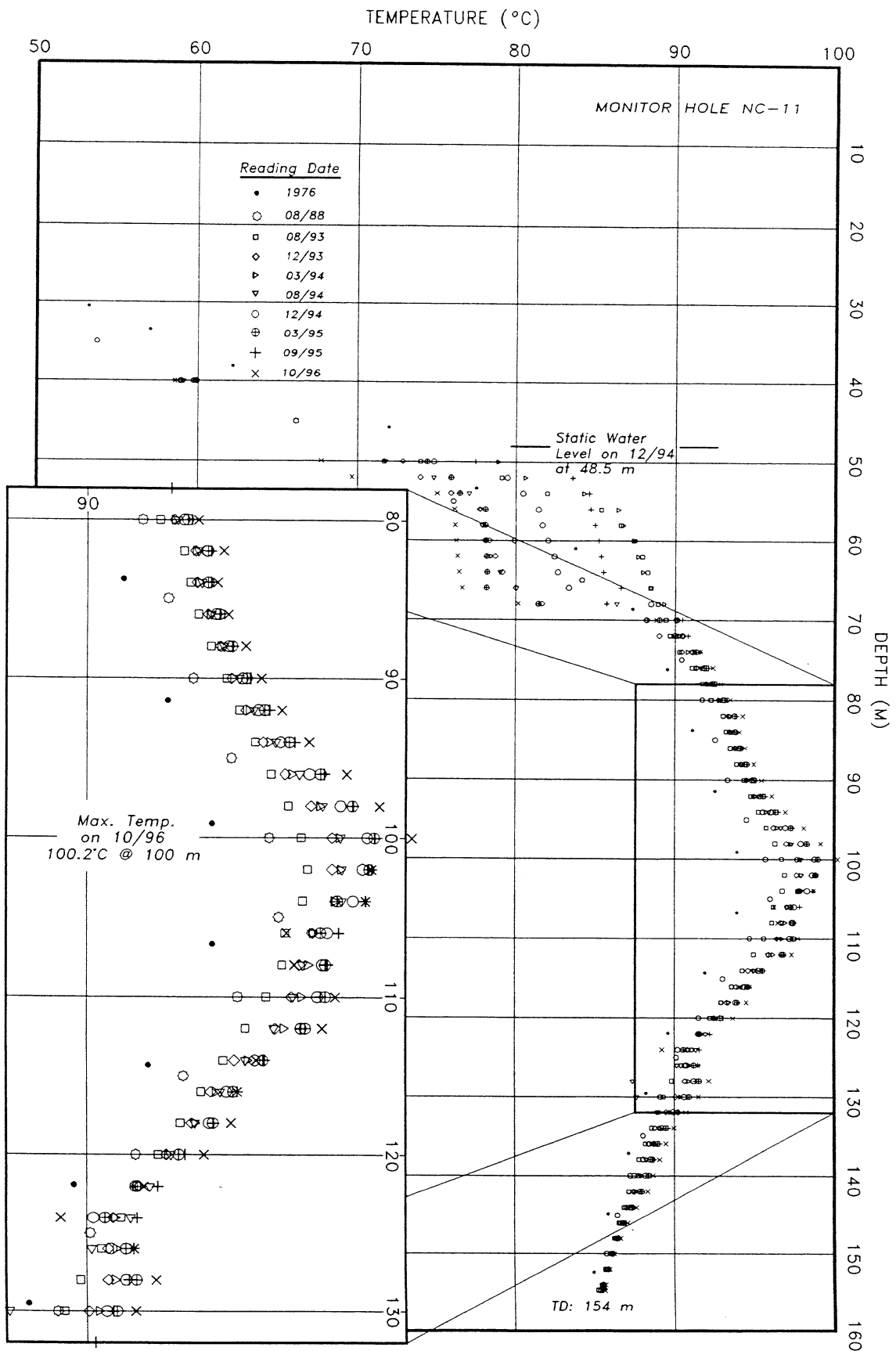


Figure 10. Temperature-depth summary for Newcastle monitor well NC-11. Plot illustrates the thermal profile based on 10 separate readings between 1976 (exact date unknown) and October 1996. Well location is shown in figure 2.

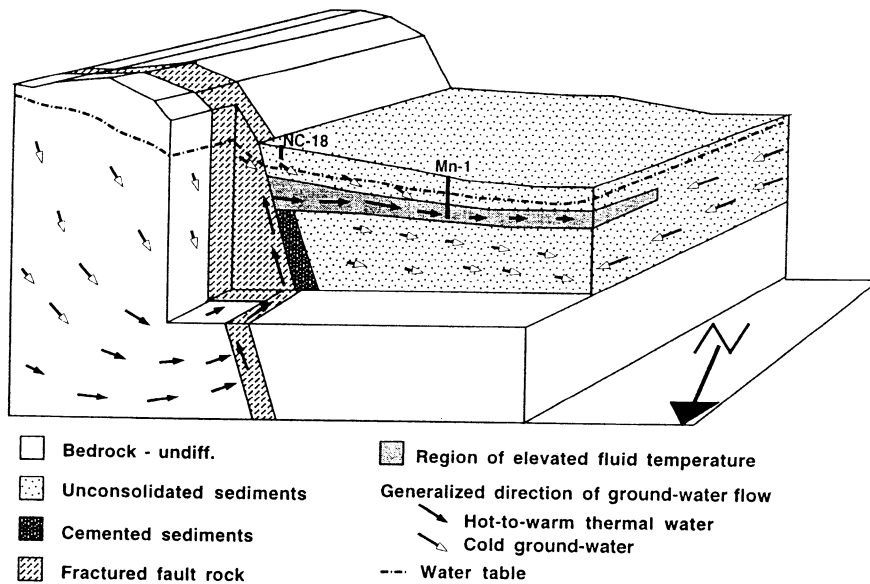


Figure 11. Conceptual model for ground-water flow in the Newcastle geothermal system (from Blackett and others, 1990).

exhibited by elevated TDS, supports the plume concept. Previous studies of the ground water regime near Newcastle (Mower, 1981, 1982) indicate a predominant northward trend for ground-water flow. This northerly pattern of flow, coupled with high heat loss from the top of the aquifer, likely causes the increasing distance between heat-flow contours found when traversing the geothermal system from south to north (figure 2). Further evidence for an elongate, northerly trending thermal-chemical plume is also provided by the chemistry and isotopic signatures of ground-water samples collected and described by Blackett and others (1990) and other ground-water samples collected by Mower (1982).

Resource Analysis

Constructing and implementing a two-dimensional, horizontal model of fluid flow and heat transfer forms an important first step in attempting to model the Newcastle geothermal system. The well-defined thermal plume shown in figure 2 provides an important set of field observations that can be used to constrain the numerical simulations. Although the Newcastle system must ultimately be simulated with a transient, three-dimensional model, a series of steady-state, two-dimensional simulations provides a sound basis for evaluating our conceptual model and testing hypotheses. In this modeling effort the objective was to establish the patterns and rates of fluid fluxes

that are required to transport heat from deep in the flow system to the observed thermal plume.

Numerical Model

A two-dimensional, finite-element model of coupled fluid flow and heat transfer in the horizontal plane was written to simulate the characteristic geometry and properties of blind geothermal systems similar to those found at Newcastle. Two coupled boundary-value problems are integrated in the model; one for fluid flow and the other for heat transfer. The simulation algorithm is a vastly modified version of the code used by Forster and Smith (1988).

A sketch of the plan-view geometry of the model domain is shown in figure 12. The aquifer of interest is assumed to be underlain by an impermeable aquitard. This requires a permeability contrast between the two units that exceeds two orders of magnitude. Insufficient data are available to test this assumption because there are no test-derived estimates of the vertical variation in permeability in the Newcastle area. The upper boundary of the Newcastle aquifer, however, is likely unconfined. Because analysis of pumping data suggests relatively high transmissivity values (on the order of 930 m² per day), water-table drawdown around pumping wells is likely only a small percentage of the aquifer thickness. Thus, it is a reasonable first approximation to assume minimal direct recharge to the aquifer and treat the aquifer as if it were effectively confined both above and below. Although the unsaturated zone that overlies the aquifer is assumed to be impermeable it does provide an important pathway for heat loss from the aquifer system. In this model ground-water recharge enters the system by horizontal flow across the aquifer boundaries and where sources are used to represent discharge from adjacent parts of the flow system. For example, recharge of water running off the mountain front and the consequences of ground-water injection and withdrawals are also included.

The surface heat-flow map shown in figure 2 provides a valuable constraint on the character of the hydrothermal flow system. These contours are superimposed on a map of the model domain in figure 12. In this example we use the heat-flow observations, and associated aquifer temperatures, to assess the ability of the numerical model to mimic the field observations.

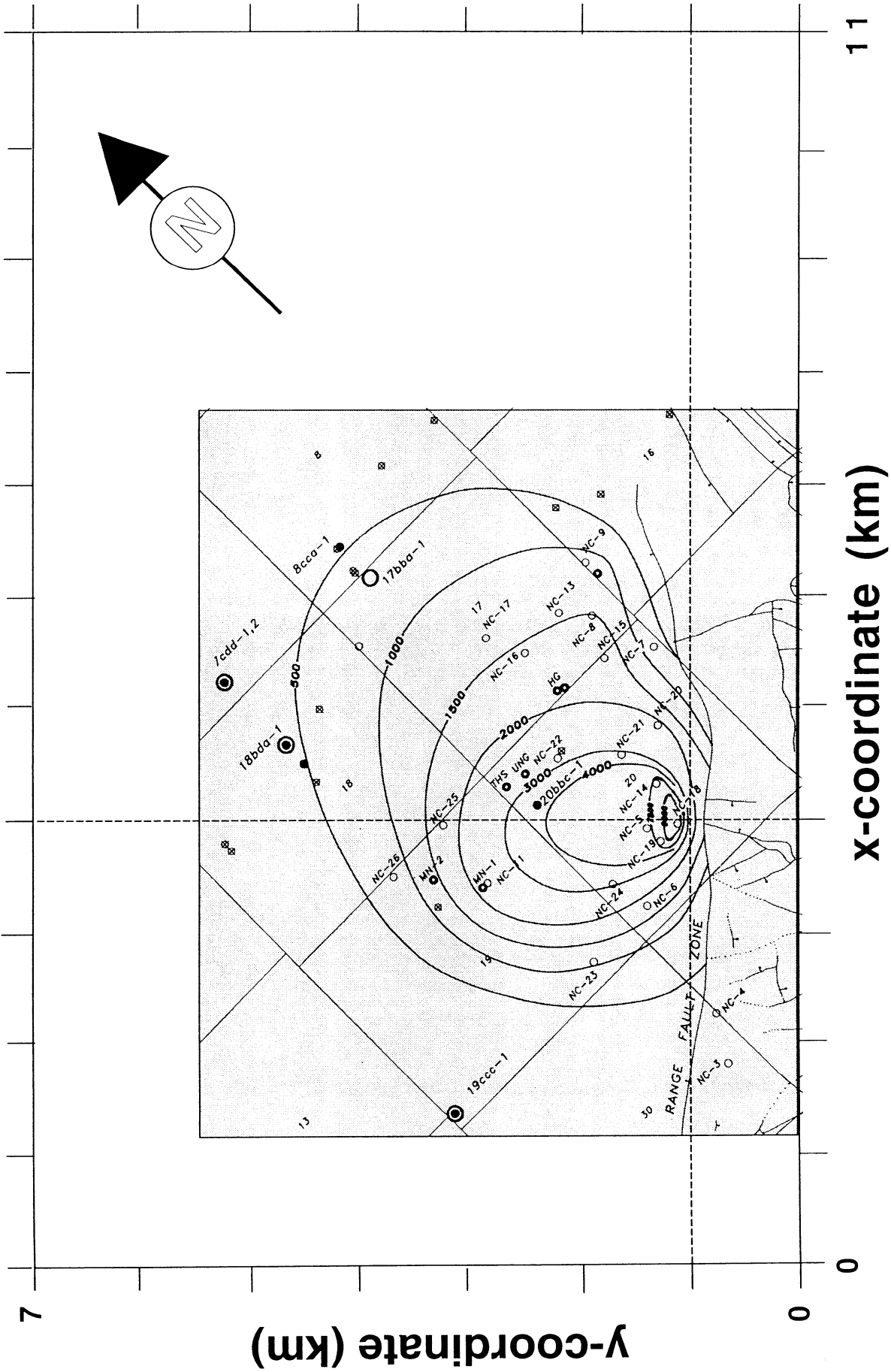


Figure 12. Numerical modeling domain and boundary conditions for two-dimensional simulations of coupled fluid flow and heat transfer at Newcastle. The dashed line parallel to the x-coordinate represents the transition from basin-fill sediments to the northwest and the adjacent mountain front to the southeast. The dashed line parallel to the y-coordinate provides a reference mark that indicates the approximate centerline of the hot core of the thermal plume. Explanation for well symbols and faults is shown on figure 2.

Although the three-dimensional model originally intended for use in the project is supposed to allow calculation of heat loss from an upper conductive layer, substantial experimentation indicated that the code is inadequate. Despite repeated attempts, the original model developers could not identify the problem. Thus, a new model was developed that would allow for conductive heat loss through the unsaturated zone so that both aquifer temperature and surface heat flow could be calculated. Surface heat flow is calculated in the model assuming uniform thermal conductivity through the upper confining layer and a linear temperature gradient between the water table and the ground surface.

The fluid-flow model resembles classical aquifer models. Spatial variations in aquifer thickness and permeability are vertically averaged and assigned to each triangular element in the finite-element grid shown in figure 13. Fluid sources and sinks represent production or injection wells by specifying the steady-state flow rate at a designated nodal position. Values of equivalent freshwater head are computed at each node and used as a basis for calculating the element-by-element values of fluid flux needed in the heat-transfer module. A confined aquifer is assumed. Constant head values may be applied both at internal nodes and along the model boundaries. The default boundary condition is one of no fluid flow (impermeable). An internal grid generator is used to construct rectangular domains with right-triangular elements.

The heat-transfer module accounts for heat transport within a confined aquifer by both conduction and advection. Spatial variations in thermal conductivity are verti-

cally averaged and assigned to each triangular element in the model grid. Although conductive heat sources and sinks can be represented at designated nodal positions, this feature was incorporated only to facilitate model validation. Advective heat transfer is included using the values of heat flux computed in the fluid-flow module. Conductive heat loss through the unsaturated zone that overlies the aquifer is calculated using the estimated thickness and thermal conductivity of the unsaturated zone combined with the difference between the aquifer and the mean annual air temperature. A uniform, estimated regional heat flow can be applied to the base of the aquifer. Where fluid sources or sinks (that is, production or injection wells) are specified, corresponding advective heat sources and sinks are included in the model.

Thermal and fluid-flow regimes are computed in an iterative process that alternately calculates fluid fluxes, updates the fluid temperatures by calculating heat fluxes, then uses the new thermal regime to re-calculate fluid fluxes. This procedure continues until little change in the character of the thermal and fluid-flow regimes is computed from one iteration to the next. Fluid properties are computed as a function of temperature and pressure using an algorithm developed by Charles W. Mase while at the University of British Columbia and incorporated in previous numerical models by Forster and Smith (1988). The numerical model was validated in both one-dimensional and two-dimensional modes using analytical solutions developed by various authors (for example, Carslaw and Jaeger, 1959; Ogata and Banks, 1961) to solve problems in conductive and advective transport of heat and solutes.

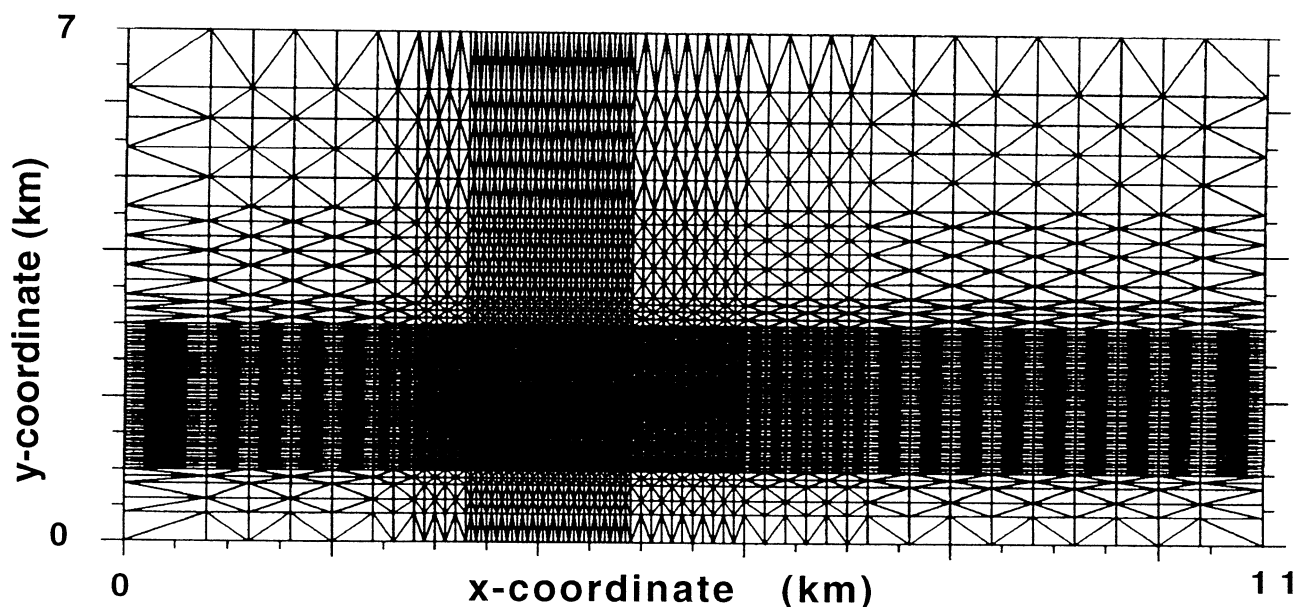


Figure 13. Finite-element mesh used in numerical simulations.

Model Geometry and Input Parameters

Finite-Element Grid

A 7 kilometers by 11 kilometers rectangular model domain is used to simulate the Newcastle system (figure 13). The grid of triangular finite elements is oriented so that the boundary between valley-fill sediments and the lower permeability bedrock that forms the mountain front is parallel to one of the model boundaries. The grid is refined with x and y spacing of 50 m in the region where heat flow is estimated to exceed 2 W m^{-2} . Progressively coarser grid sizes (100, 200, 400, 600, and 800 m grid spacing) surround the fine-grid region. A relatively large model domain is selected in order to minimize the influence of the poorly known boundary conditions on the model results.

Boundary Conditions and Aquifer Recharge

In the fluid-flow module constant-head values are applied at each boundary node. Values are selected in an effort to produce a plausible regional-scale flow system with dominant directions suggested by water levels measured in wells and inferred from local topography, groundwater chemistry, and ground-water temperatures. For example, water-level data, fluid chemistry, and fluid temperature suggest ground water in the local area is moving predominantly to the north. Linearly varying head distributions are assigned along each boundary in an effort to capture this generalized flow direction.

Values of head specified at each corner are shown in figure 14. Relatively high head values are assigned along the mountain front in an effort to represent the higher heads found in the lower permeability bedrock. Several different head distributions were tested until the one shown in figure 14 was adopted. This pattern provides the driving force needed to produce the northeastward drift of the thermal plume while counterbalancing the northwestward driving forces provided by fluid sources specified along the mountain front.

Points of fluid injection (figure 14) are also specified along the mountain front to represent recharge to the aquifer from surface runoff generated in the adjacent mountains and discharge from deeper parts of the flow system. Note that the fluid injection rates shown in figure 14 are the values applied at each node (figure 13) within the appropriately shaded regions of figure 14, rather than an average rate of recharge specified along the distance indicated by each shaded region. In the final simulation series, a point withdrawal is added to the model to represent the production of thermal fluid at the Milgro Nursery (MN-1).

The total influx of hot water specified along the mountain front is 114 kg s^{-1} ($0.11 \text{ m}^3 \text{ s}^{-1}$). An additional influx of about 7 kg s^{-1} ($7 \times 10^{-3} \text{ m}^3 \text{ s}^{-1}$) of cold water is also specified. The total recharge of 121 kg s^{-1} ($0.13 \text{ m}^3 \text{ s}^{-1}$) could be supplied by an annual rainfall of 1 cm per year within a watershed area approximately 100 km^2 . This recharge rate is consistent with the field situation at Newcastle because annual rainfall is higher than 1 cm per year over watershed areas in the adjacent Pine Valley Mountains and Antelope Range. The fluid fluxes specified as recharge sources in the model yield a localized source of hot ground water that forms the thermal plume. Chapman and others (1981) used the heat-flow map to estimate that $0.031 \text{ m}^3 \text{ s}^{-1}$ of hot fluid discharging to the aquifer may cause the observed thermal plume. Given the uncertainties inherent in each approach, this factor of four difference in estimated fluid recharge is acceptable.

In the heat-transfer module a constant, uniform temperature of 15°C is applied at each boundary node. For convenience the boundary temperatures are also assumed equal to the mean annual air temperature. Specified temperature nodes (shaded region shown in figure 14) are used to generate the elevated temperatures (estimated at 130°C) associated with the inferred region of up-flowing hot water. The basal heat-flow option is not invoked because temperature-depth profiles indicate approximately isothermal conditions beneath the aquifer of interest. Thus, little heat is lost or gained from the base of the aquifer. Heat lost through the upper surface of the aquifer is, however, computed during the simulations.

Material Properties

Material properties are assigned uniformly within each of the six regions shown in figure 15. Parameter values are outlined in table 1. The values shown in table 1 reflect the results of at least 40 attempts to mimic the field-based pattern of surface heat flow and aquifer temperature with the computed results. Unfortunately the model results are highly sensitive to parameters for which few data exist. For example, both the aquifer thickness and the thickness of the unsaturated zone (roughly the depth to the water table) are poorly constrained. Although permeabilities used in the model are consistent with the values suggested by Mower (1982), our sensitivity studies reveal that relatively small changes in absolute value and degree of anisotropy can create important changes in the computed thermal regime. Thus, the values used in the model are only one of many sets of possible parameter values that might produce results similar to the field-based observations. The following paragraphs outline the basis used to select the model parameters.

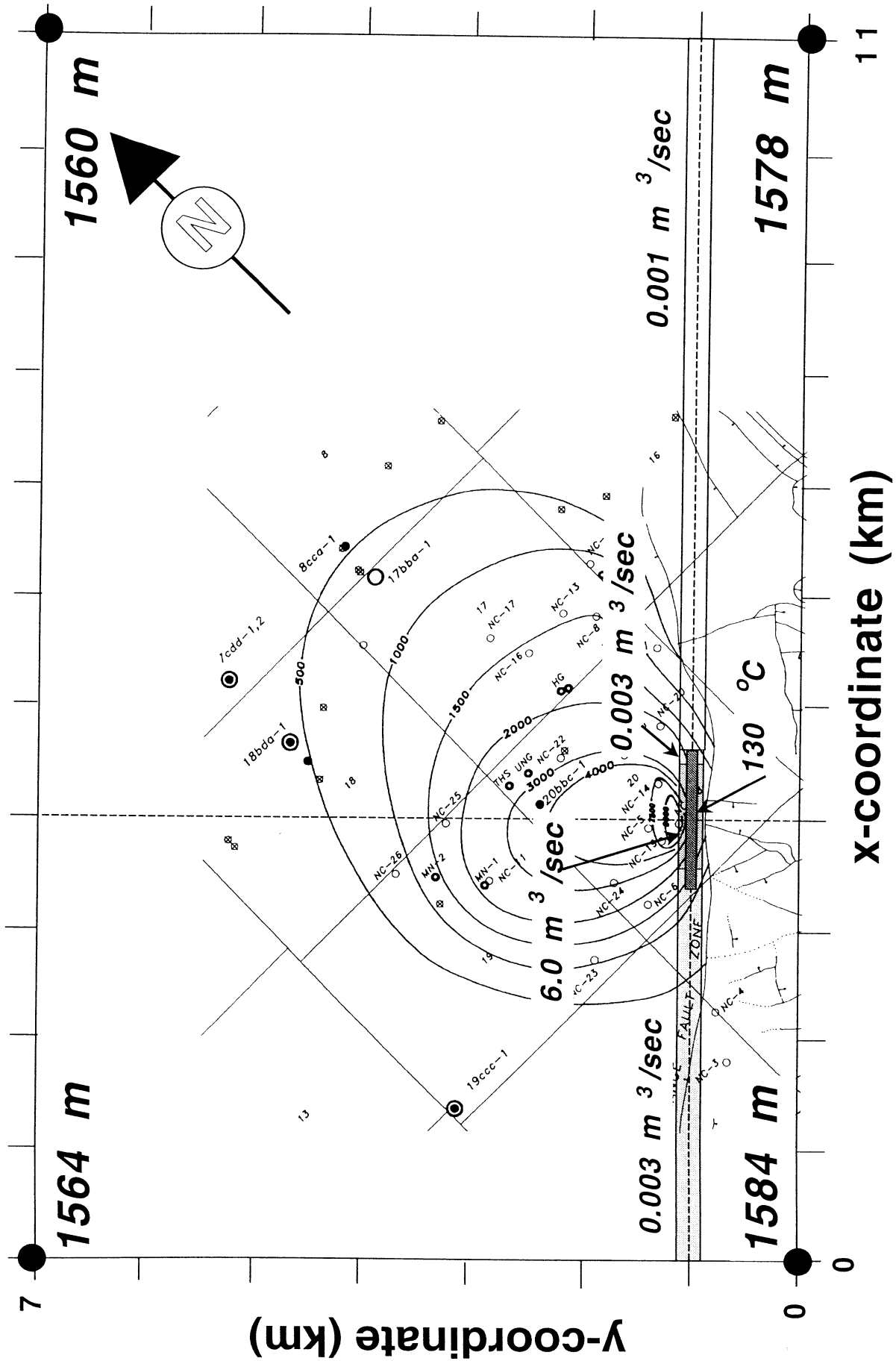


Figure 14. Boundary conditions applied to solve the coupled fluid-flow and heat-transfer boundary value problem. A constant temperature of 15°C is assigned around the model perimeter and to the ambient air temperature. Linearly varying values of hydraulic head are assigned along each side of the model domain between the head values noted at each corner of the domain. Explanation for well symbols and faults is shown on figure 2.

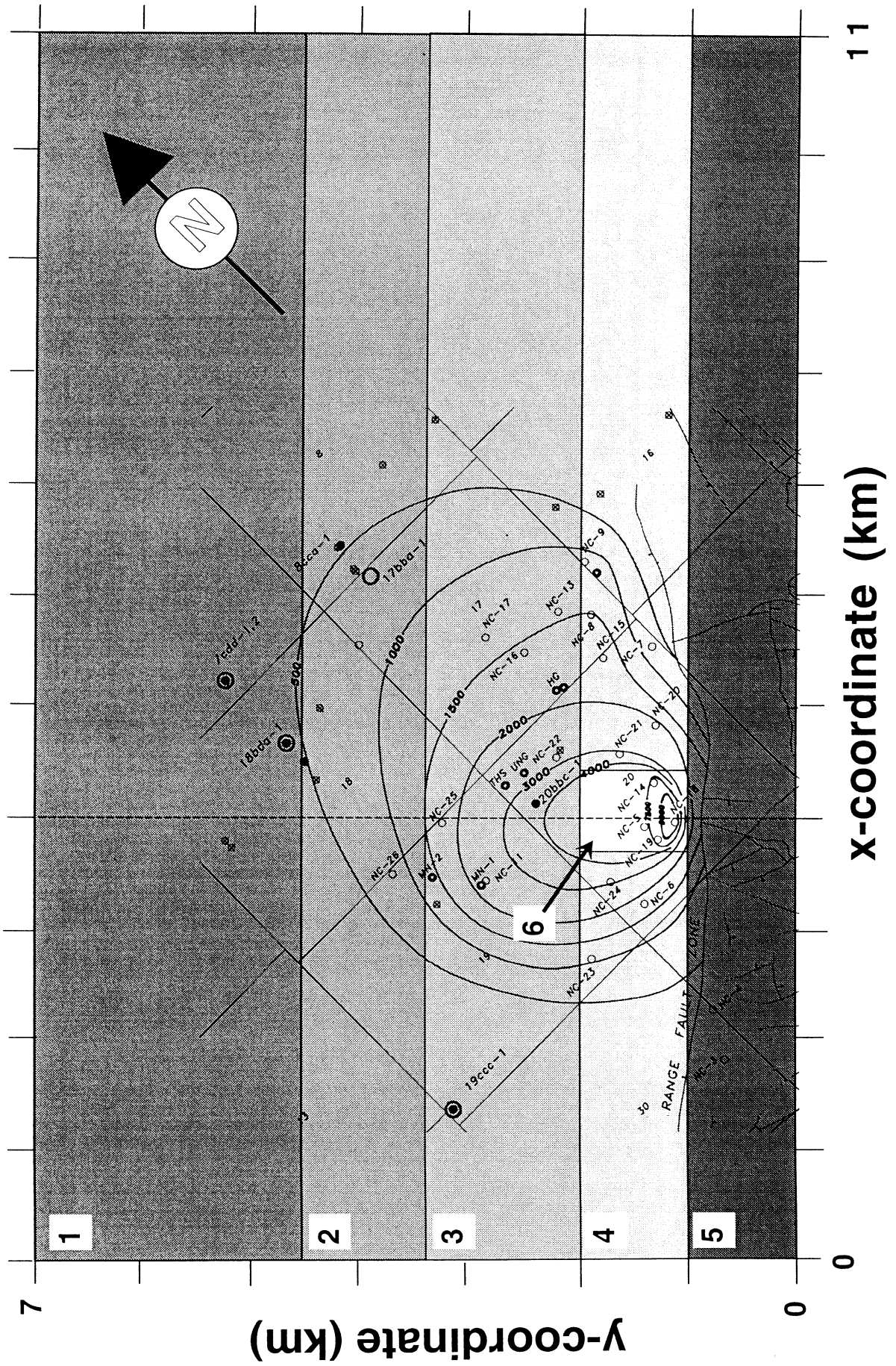


Figure 15. Areas assigned material property values listed in table 1. Explanation for well symbols and faults is shown on figure 2.

Mower (1982) infers that aquifer transmissivity in the vicinity of the thermal plume may be on the order of $0.0107 \text{ m}^2 \text{ s}^{-1}$. In the absence of the drilling information needed to estimate aquifer thickness we have assumed a constant thickness of 35 m. This estimate is based primarily on inspection of temperature-depth profiles measured in wells that penetrate the entire aquifer. An isothermal region is typically found between depths of about 75 to 110 m. Dividing this thickness into the estimated transmissivity suggests that hydraulic conductivity values may be on the order of $3.07 \times 10^{-4} \text{ m s}^{-1}$. This yields an aquifer permeability on the order of $3 \times 10^{-11} \text{ m}^2$. This value is consistent with the fact that the unconsolidated deposits that make up the aquifer comprise sand and gravel. No information is available to estimate permeability anisotropy; however, since alluvial deposits are normally shed away (perpendicular) from the mountain front, we reasonably assume that permeability measured in a direction parallel to the mountain front will be somewhat reduced relative to that measured in a perpendicular direction.

In attempting to compute a thermal plume that resembles the one shown in figure 2, permeability values used in the model (table 1) are set between 10^{-11} and 10^{-16} m^2 . Given the lack of permeability testing information and inherent uncertainties in estimating aquifer thickness, these permeability values appear reasonable. In attempting to control the length and northeastward drift of the plume, a small degree of permeability anisotropy (see values of k_x and k_y in table 1) was found to be advantageous.

Because bedrock permeability is likely to be several orders of magnitude lower than that of the basin-fill deposits, the model is very insensitive to the value assigned to unit 5 (table 1, figure 15). The value chosen is representative of moderately fractured rock with low matrix permeability.

Thermal conductivity values are based on measurements and estimates made by Blackett and others (1990). Porosity values are estimated to be consistent with the geologic material. Insufficient information is available to consider assigning anything other than uniform values for

each general category, bedrock and unconsolidated deposits. Thermal conductivity of the unsaturated zone that overlies the aquifer is reduced from 1.7 to $1.2 \text{ W m}^{-1} \text{ K}^{-1}$ (thermal conductivity units are in watts per meter-Kelvin) to account for the higher thermal resistance of air filling the pore space.

Simulation results were found to be highly sensitive to the estimated thickness of the unsaturated zone. Although computed surface heat flow is directly proportional to the thickness, little information is available to constrain thickness variability within the modeling domain. Several difficult-to-estimate factors control the effective thickness that must be assigned in the model. For example, where a steam plume is inferred to yield the maximum heat flow-values (well NC-18 in figure 2), the effective thickness of the unsaturated zone is likely to be the distance between the ground surface and the top of the steam plume, rather than the deeper water table. Elsewhere, the depth to the water table is controlled by changes in surface topography and the character of the ground-water flow system. Because thickness of the unsaturated zone could vary by up to a factor of five within the model domain, a similar range in uncertainty must be accorded the computed estimates of surface heat flux. In performing the numerical sensitivity studies we observed that the computed aquifer temperature was strongly controlled by the estimated thickness of the unsaturated zone because the primary mechanism for heat loss from the aquifer is through the overlying unsaturated zone.

Modeling Results

Preliminary modeling results using the FEHMN (finite element heat and mass transfer) code (Zyvoloski and others, 1992) indicated that we should include the process of heat leakage from the top of the aquifer to the ground surface in the numerical model. After experimenting with the FEHMN code we concluded that the code would not operate in the desired mode.

Results obtained using the new code, with input values shown in table 1, are shown in figures 16a and 16b.

Table 1. Parameter values used in final simulation.

Unit	Permeability		Thermal Conductivity (W/mK)	Porosity %	Thickness (m)	
	k_x (m^2)	k_y (m^2)			Aquifer	Unsaturated Zone
1	1×10^{-11}	1×10^{-11}	1.7	0.3	35	20
2	5×10^{-11}	6×10^{-11}	1.7	0.3	35	20
3	6×10^{-11}	8×10^{-11}	1.7	0.3	35	25
4	5×10^{-11}	7×10^{-11}	1.7	0.3	35	25
5	1×10^{-16}	1×10^{-16}	2.6	0.1	35	200
6	7×10^{-11}	9×10^{-11}	1.7	0.3	35	14

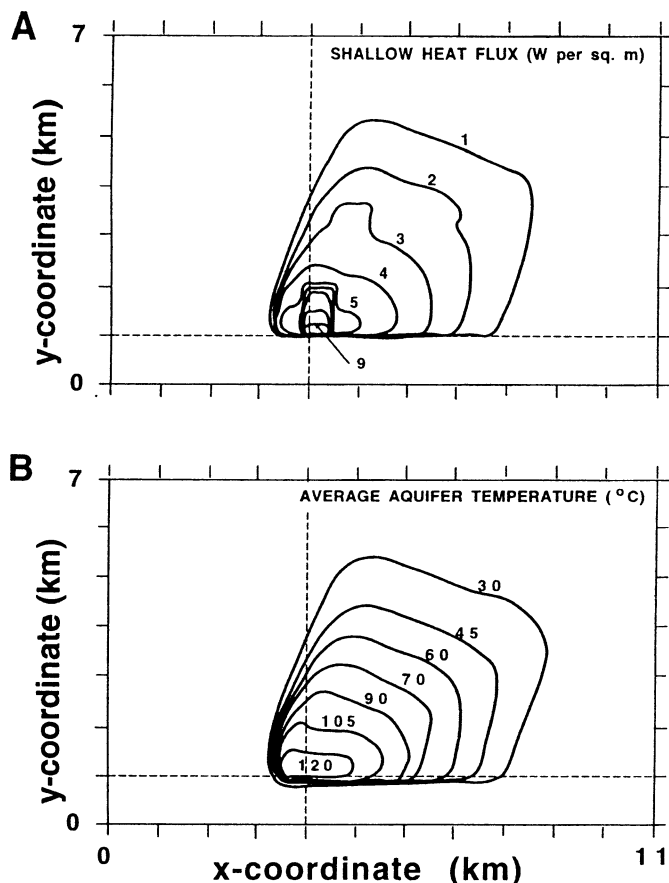


Figure 16. Simulation results: (A) computed vertical heat flow through the unsaturated zone that overlies the aquifer of interest, and (B) corresponding temperature distribution within the aquifer.

Although the match between the field-based and computed map of heat flow is poor (figure 17), the primary elements of the field problem are captured in the computed result. For example, the northeastward “drift” of the thermal plume is captured by specifying a set of boundary conditions that causes a net flow of ground water from southwest to northeast. The 1.2 km line of hot water influx nodes specified along the mountain front provides a localized source for the thermal plume and a plume area encompassed by the 1 W contour line similar to that found in the field case. Thus, it appears that the combination of aquifer permeability, aquifer thickness, and fluid recharge along the mountain front may be approximately correct.

Note that a thin unsaturated zone is required in the vicinity of NC-18 to obtain the maximum computed heat flow of 9.2 W shown in figure 16b. The large localized increase in heat flow, in excess of 9 W, reflects a local decrease in unsaturated zone thickness from 15 to 14 m. Given an aquifer temperature of 130°C and a thermal conductivity of 1.2 W m⁻¹ K⁻¹ assumed for the unsaturated zone, the heat flow estimated at NC-18 can only be

matched by assigning an unsaturated zone thickness less than 14 m. This is approximately the depth that the PVC casing reportedly deformed in the NC-18 monitor well. Although we assume that steam generated at the water table is carrying heat to shallower depths than would be anticipated, rather than the water table rising to within 15 meters of the ground surface, we lack the water-level data needed to assess this possibility.

Because the numerical results are highly sensitive to the thickness of the unsaturated zone, small changes in thickness elsewhere in the model domain could significantly modify the heat-flow pattern shown in figures 16a and 17. The sensitivity of the model to the thickness of the unsaturated zone as discussed in the previous paragraph is well illustrated in figure 16a. If a constant thickness were assumed, the resulting heat-flow pattern would be very similar to the contour map obtained for the temperature regime (figure 16b).

Insufficient data are available to warrant further, more detailed, tinkering with the parameter values in attempts to better match the field-based thermal regime. The numerical results suggest that our conceptual model is reasonable.

Given the parameter values shown in table 1, direct comparison of the total mass flux of hot fluid assigned to enter the model domain (114 kg s⁻¹) with the estimated annual discharge from the primary Milgro production well (32.7 kg s⁻¹, Bill Gordon, Milgro Nurseries, verbal communication, 1996) suggests that current production levels of geothermal fluid may have significant long-term effects on the thermal regime. Recall that Clement (1981) and Rush (1983), using analytical approaches, estimated a mass flow of roughly 30 kg s⁻¹ of hot fluid into the aquifer from the source zone - about equal to current production levels. Estimating the short-term influence of pumping wells on the size and geometry of the thermal plume would require a transient simulator. Other scenarios that include a thinner, higher permeability aquifer might also create a different impact. Additional data regarding variations in aquifer thickness, thickness of the unsaturated zone, permeability, water level, and aquifer temperatures are required before these issues can be more fully evaluated. Efforts to evaluate the future impact of additional geothermal wells would be best accomplished using a transient version of the current model. Information regarding current and projected pumping rates for all wells (both cold and hot water supply wells) located within the model domain would also be required.

Conclusions

The general character of the thermal regime observed at Newcastle has been studied using a new, two-dimen-

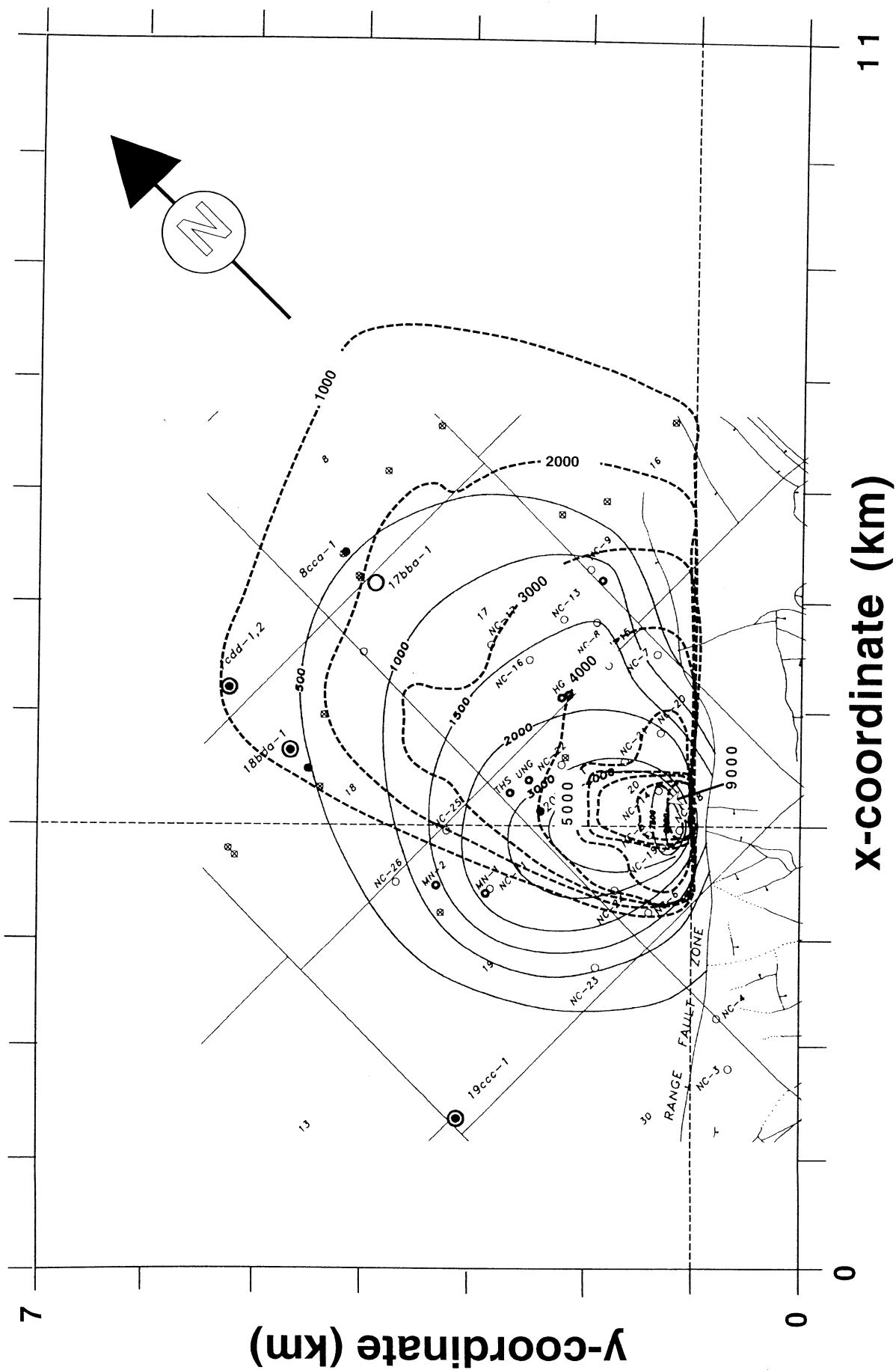


Figure 17. Comparison of computed (dashed contours) and observed (solid contours) thermal plumes ($mW m^{-2}$). Explanation for well symbols and faults is shown on figure 2.

sional fluid-flow and heat-transfer simulator. Computed aquifer temperature and surface heat-flow regimes loosely resemble those of the thermal plume mapped in the field. Parameter values, fluid recharge values, and boundary conditions assigned in the model appear to be consistent with our level of knowledge of the Newcastle geothermal system and the surrounding hydrogeological regime. Thus, the model results suggest that our conceptual model for the geothermal system shown in figure 11 is reasonable.

The simulation results are strongly influenced by aquifer permeability, thickness, and the thickness of the overlying unsaturated zone. The unsaturated-zone thickness is a critical factor in determining aquifer temperature and surface heat flow. Limited information is available to assess the spatial variability in each of these parameters at the Newcastle geothermal system. Consequently, it is unwarranted (and likely impossible) to match a computed thermal regime to the field-based observations without additional data.

The steady-state numerical model used in this study likely provides a reasonable basis for assessing the long-term impact of current and projected geothermal development at the Newcastle geothermal area. Initial simulations suggest that current geothermal development may have long-term impact on the character and geometry of the thermal plume. Additional field-based data are required to refine this conclusion. A transient version of the model, however, is needed to better assess the potential for shorter term interference between production wells. Although a three-dimensional model would better represent the sources of fluid recharge approximated as fluid sources in the two-dimensional model, sufficient data are unlikely to become available to make a three-dimensional model a valuable predictive tool. A transient version of the two-dimensional model, however, should provide valuable insight.

Recommendations

Two categories of recommendations may improve estimates of resource potential. The first category consists of collecting additional field-based data while the second category consists of refinements to the numerical modeling strategy.

Additional data should be collected to outline possible

variations in the thickness of the unsaturated zone by measuring water levels in all available wells. Vertical variations in grain size within the unconsolidated deposits should be estimated from new and existing monitor wells in an effort to obtain improved constraints on aquifer thickness and permeability. A comprehensive survey of aquifer temperature should be carried out to update and refine the distribution of ground-water temperature within and near the thermal plume. Although advantageous, detailed temperature logging is not required in all wells; rather, temperature logging is most important to obtain an estimate of the average aquifer temperature.

A more comprehensive analysis of the geothermal resource potential at Newcastle should be carried out using a transient version of the model applied in this study. When coupled with additional data constraints, a transient model would provide insight into the possible short-term interference between current and projected geothermal production wells. Temperature-depth profiles previously collected by the Utah Geological Survey over a three-year period provide a good database for calibrating the transient model to the effects of geothermal production from operators at Newcastle.

Recommendations include: (1) drilling three new monitor wells at strategic locations, (2) lithologic studies using well cuttings, and (3) aquifer tests to provide data for a numerical model which could predict aquifer response under increased pumping levels. Also recommended is an expanded effort in temperature and water-level monitoring, but at a reduced frequency of once every two or three months during the greenhouse heating season. These activities would require new funding and such funding has not yet been identified.

ACKNOWLEDGMENTS

This work was supported, in part, by the U.S. Department of Energy through Idaho National Engineering Laboratory Subcontract No. C87-101314 to the Energy and Geoscience Institute, University of Utah and through an Oregon Institute of Technology subcontract to the Utah Geological Survey. Such support does not constitute an endorsement by the U.S. Department of Energy of the views expressed in this document.

REFERENCES

- Anderson, R.E., and Christenson, G.E., 1989, Quaternary faults, folds, and selected volcanic features, Cedar City 1° x 2° quadrangle, Utah: Utah Geological and Mineral Survey Miscellaneous Publication 89-6, scale 1:250,000.
- Blackett, R.E., 1993, Temperature-gradient monitoring study, Newcastle geothermal area, Iron County, Utah: Utah Geological Survey unpublished technical report, December 7, 9 p.
- 1994, Temperature-gradient monitoring study, Newcastle geothermal area, Iron County, Utah: Utah Geological Survey unpublished technical report, March 14, 9 p.
- Blackett, R.E., and Shubat, M.A., 1992, A case study of the Newcastle geothermal system, Iron County, Utah: Utah Geological Survey Special Study 81, 30 p.
- Blackett, R.E., Shubat, M.A., Chapman, D.S., Forster, C.B., Schlinger, C.M., and Bishop, C.E., 1990, The Newcastle geothermal system, Iron County, Utah—geology, hydrology, and conceptual model: Utah Geological Survey Open-File Report No. 189, 179 p.
- Carlsaw, H.S., and Jaeger, J.C., 1959, Conduction of heat in solids: Oxford, Clarendon Press, Second Edition, 510 p.
- Chapman, D.S., Clement, M.D., and Mase, C.W., 1981, Thermal regime of the Escalante Desert, Utah, with an analysis of the Newcastle geothermal system: *Journal of Geophysical Research*, v. 86, no. B12, p. 11,735-11,746.
- Clement, M.D., 1981, Heat flow and geothermal assessment of the Escalante Desert, part of the Oligocene to Miocene Volcanic Belt in Southwestern Utah: Salt Lake City, University of Utah Department of Geology and Geophysics, M.S. thesis, 118 p.
- Forster, C.B., and Smith, Leslie, 1988, Groundwater flow systems in mountainous terrain, 2, controlling factors: *Water Resources Research*, v. 24, no. 7, p. 1011-1023.
- Mower, R.W., 1981, Ground-water data for the Beryl-Enterprise area, Escalante Desert, Utah: U.S. Geological Survey Open-File Report 81-340, 64 p.
- 1982, Hydrology of the Beryl-Enterprise area, Escalante Desert, Utah, with emphasis on ground water: State of Utah, Department of Natural Resources Technical Publication 73, 66 p.
- Ogata, Akio, and Banks, R.B., 1961, A solution of the differential equation of longitudinal dispersion in porous media: U.S. Geological Survey Professional Paper 411-A, p. A1-A7.
- Pe, Win, and Cook, K.L., 1980, Gravity survey of the Escalante Desert and vicinity, in Iron and Washington Counties, Utah: Salt Lake City, University of Utah, Department of Geology and Geophysics Report no. DOE/ID/12079-14, 156 p.
- Ross, H.P., Blackett, R.E., Forster, C.B., and Snelgrove, Stephen, 1994, A model for sustainable development - the Newcastle, Utah geothermal resource, in Blackett, R.E., and Moore, J.N., editors, Cenozoic geology and geothermal systems of southwestern Utah: Salt Lake City, Utah Geological Association Publication 23, p. 69-79.
- Ross, H.P., Blackett, R.E., Shubat, M.A., and Mackelprang, C.E., 1990, Delineation of fluid up-flow and outflow plume with electrical resistivity and self-potential data, Newcastle geothermal area, Utah: *Geothermal Resources Council Transactions*, v. 14, p. 1,531-1,536.
- Rush, F.E., 1977, Subsurface-temperature data for some wells in western Utah: U.S. Geological Survey Open-File Report 77-132, 36 p.
- 1983, Reconnaissance of the hydrothermal resources of Utah: U.S. Geological Survey Professional Paper 1044-H, 49 p.
- Shubat, M.A., and Siders, M.A., 1988, Geologic map of the Silver Peak quadrangle, Iron County, Utah: Utah Geological and Mineral Survey Map 108, 13 p., scale 1:24,000.
- Siders, M.A., Rowley, P.D., Shubat, M.A., Christenson, G.E., and Galyardt, G.L., 1990, Geologic map of the Newcastle quadrangle, Iron County, Utah: U.S. Geological Survey Geologic Quadrangle Map GQ-1690, scale 1:24,000.
- Zyvoloski, G.A., Dash, Zora, and Kelkar, Sharad, 1992, FEHMN 1.0 - Finite element heat and mass transfer code: Los Alamos National Laboratory Report LA-12062-MS, Revision 1, 113 p.

APPENDIX

Temperature-Gradient Data for Monitor Wells NC-7, NC-9, NC-11, NC-13, and NC-15.

MONITOR WELL NC-11

	08/31/93	10/6/93	11/02/93	12/03/93	01/06/93	02/06/94	03/07/94	04/11/94	05/09/94	08/30/94	12/5/94	03/23/95	09/11/95	10/17/96	Cumul.
Depth	Temp.	Temp.	Temp.	Temp.	Temp.	Temp.	Temp.	Temp.	Temp.	Temp.	Temp.	Temp.	Temp.	Temp.	Diff.
(m)	(°C)	(°C)	(°C)	(°C)	(°C)	(°C)	(°C)	(°C)	(°C)	(°C)	(°C)	(°C)	(°C)	(°C)	(°C)
20.0	38.8	40.2	32.6	28.6	35.3	36.2	38.3	33.7	33.9	40.4	38.0	41.1	36.6	33.9	-4.9
40.0	59.9	60.0	59.6	58.9	59.6	59.6	59.8	59.4	59.2	59.1	58.9	59.9	60.0	58.5	-1.4
50.0	74.0	74.6	75.3	72.9	76.6	77.4	78.9	79.7	76.7	71.8	74.9	74.5	77.5	67.7	-6.3
52.0	79.1	76.6	76.2	74.1	77.6	79.1	80.6	81.3	77.9	74.9	79.5	75.9	83.5	69.6	-9.5
54.0	81.9	79.2	78.5	76.0	80.1	82.6	84.2	84.8	80.6	77.1	80.5	76.5	84.5	75.1	-6.8
56.0	85.3	81.6	79.5	77.7	80.3	85.1	86.4	86.8	82.1	77.8	81.4	78.1	84.6	76.1	-9.2
58.0	86.6	83.7	79.7	77.9	80.5	85.5	86.6	87.1	82.6	77.9	81.7	78.1	84.9	76.2	-10.3
60.0	87.4	85.7	80.4	78.4	81.1	86.3	87.4	87.7	83.5	78.1	82.0	78.1	85.2	76.3	-11.1
62.0	87.9	86.7	81.1	78.7	81.5	86.7	87.6	87.8	84.2	78.4	82.4	78.2	85.3	76.4	-11.5
64.0	88.2	87.5	81.8	79.2	82.1	87.0	87.9	88.1	85.1	79.0	82.6	78.2	85.5	76.4	-11.8
66.0	88.4	88.2	83.0	80.0	82.6	87.8	88.4	88.6	86.2	80.1	83.3	78.2	86.5	76.6	-11.8
68.0	88.9	87.9	84.8	81.7	84.4	88.6	89.3	89.3	88.4	86.3	88.4	81.4	85.7	80.2	-8.8
70.0	89.4	89.3	89.0	88.1	88.4	89.9	90.0	90.1	90.1	90.0	90.1	89.0	90.5	88.8	-0.6
72.0	89.6	89.6	89.6	89.0	89.2	90.1	90.3	90.4	90.4	90.4	90.5	90.0	90.8	90.0	0.3
74.0	90.2	90.3	90.4	90.4	90.4	90.6	90.8	90.8	90.8	91.0	91.1	91.3	91.5	91.6	1.3
76.0	91.0	91.2	91.2	91.3	91.4	91.4	91.4	91.5	91.5	91.6	91.8	92.0	92.1	92.4	1.3
78.0	91.7	91.8	91.9	92.0	92.0	92.0	92.0	92.0	92.0	92.1	92.3	92.5	92.6	92.9	1.1
80.0	92.3	92.5	92.6	92.7	92.7	92.7	92.7	92.7	92.6	92.8	93.0	93.1	93.3	93.5	1.2
82.0	93.0	93.2	93.3	93.3	93.4	93.4	93.3	93.3	93.3	93.5	93.7	93.7	93.8	94.2	1.3
84.0	93.2	93.3	93.4	93.4	93.5	93.5	93.5	93.5	93.5	93.6	93.7	93.7	93.9	94.1	0.8
86.0	93.5	93.6	93.7	93.7	93.8	93.8	93.8	93.8	93.8	93.8	94.0	94.1	94.2	94.4	1.0
88.0	93.9	94.0	94.1	94.2	94.2	94.2	94.2	94.2	94.2	94.2	94.4	94.5	94.6	94.9	1.1
90.0	94.3	94.4	94.5	94.5	94.6	94.6	94.6	94.6	94.6	94.8	94.8	95.0	95.1	95.5	1.1
92.0	94.8	94.8	94.9	94.9	95.0	95.0	95.0	95.1	95.0	95.2	95.4	95.6	95.7	96.1	1.3
94.0	95.3	95.3	95.5	95.5	95.6	95.7	95.7	95.8	95.8	95.9	96.0	96.3	96.5	96.9	1.7
96.0	95.8	95.9	96.0	96.2	96.3	96.4	96.4	96.5	96.4	96.6	96.9	97.3	97.4	98.1	2.4
98.0	96.3	96.5	96.7	97.0	97.1	97.2	97.2	97.2	97.2	97.3	97.9	98.3	98.3	99.1	2.9
100.0	96.7	97.1	97.3	97.7	97.9	97.9	97.9	97.9	97.9	97.9	98.8	99.0	99.0	100.2	3.5
102.0	96.9	97.1	97.4	97.7	97.9	97.9	97.9	97.9	98.0	97.9	98.6	98.8	98.9	98.9	2.0
104.0	96.7	97.4	97.7	97.8	97.8	97.7	97.7	97.8	97.8	98.0	98.3	97.8	98.7	98.7	2.0
106.0	96.2	96.7	96.9	97.0	97.1	97.1	97.0	97.0	97.1	97.0	97.5	97.3	97.9	96.2	0.0
108.0	96.1	96.1	96.4	96.6	96.8	96.8	96.9	96.9	96.9	96.7	97.3	97.4	97.5	96.5	0.4
110.0	95.6	95.9	96.1	96.4	96.6	96.7	96.7	96.7	96.7	96.4	97.2	97.4	97.3	97.8	2.2
112.0	94.9	95.5	95.7	95.9	96.1	96.1	96.1	96.2	96.2	95.8	96.7	96.8	96.7	97.3	2.4
114.0	94.2	94.3	94.6	94.6	94.9	94.8	95.0	95.0	95.1	94.9	95.3	95.5	95.6	95.3	1.1
116.0	93.6	93.6	93.7	93.8	93.9	94.0	94.0	94.1	94.2	94.2	94.3	94.6	94.7	94.7	1.1
118.0	92.9	93.0	93.2	93.3	93.3	93.3	93.3	93.5	93.5	93.3	93.8	93.9	94.0	94.5	1.6
120.0	92.2	92.3	92.4	92.5	92.6	92.5	92.5	92.6	92.6	92.6	92.9	92.9	93.0	93.7	1.5
122.0	91.6	91.5	91.6	91.6	91.7	91.6	91.7	91.7	91.8	92.0	91.6	91.5	92.2	91.7	0.2
124.0	91.0	90.8	90.9	90.8	90.8	90.8	90.9	91.0	91.2	91.4	90.2	90.6	91.5	89.2	-1.8
126.0	90.4	90.4	90.6	90.7	90.8	90.9	90.9	91.0	91.0	90.2	90.8	91.2	91.5	91.5	1.0

Monitor Well NC-11 (continued)

	08/31/93	10/6/93	11/02/93	12/03/93	01/06/93	02/06/94	03/07/94	04/11/94	05/09/94	08/30/94	12/5/94	03/23/95	09/11/95	10/17/96	Cumul.
Depth	Temp.	Temp.	Temp.	Temp.	Temp.	Temp.	Temp.	Temp.	Temp.	Temp.	Temp.	Temp.	Temp.	Temp.	Diff.
(m)	(°C)	(°C)	(°C)	(°C)	(°C)	(°C)	(°C)	(°C)	(°C)	(°C)	(°C)	(°C)	(°C)	(°C)	(°C)
128.0	89.8	90.2	90.4	90.6	90.8	90.8	90.9	91.0	90.9	87.3	91.2	91.5	91.3	92.2	2.4
130.0	89.3	89.6	89.9	90.0	90.3	90.3	90.4	90.4	90.4	87.6	90.6	90.9	90.8	91.5	2.2
132.0	89.0	89.1	89.3	89.5	89.6	89.6	89.7	89.8	89.8	88.9	89.9	90.2	90.2	90.7	1.8
134.0	88.5	88.6	88.7	88.7	89.0	89.0	89.0	89.1	89.2	89.0	89.1	89.5	89.6	90.0	1.4
136.0	88.1	88.2	88.3	88.4	88.5	88.5	88.5	88.6	88.7	88.7	88.7	88.9	89.1	89.5	1.3
138.0	87.8	87.8	88.0	88.0	88.1	88.2	88.2	88.2	88.3	88.2	88.4	88.6	88.7	89.0	1.3
140.0	87.5	87.5	87.7	87.7	87.8	87.9	87.9	88.0	88.0	87.8	88.1	88.4	88.3	88.7	1.2
142.0	87.1	87.2	87.3	87.4	87.6	87.6	87.6	87.6	87.6	87.5	87.8	88.0	87.9	88.3	1.2
144.0	86.8	86.8	86.9	87.0	87.0	87.0	87.1	87.1	87.1	87.1	87.2	87.3	87.4	87.6	0.8
146.0	86.5	86.5	86.6	86.6	86.7	86.6	86.6	86.7	86.7	86.7	86.8	86.8	87.0	87.1	0.5
148.0	86.2	86.2	86.3	86.3	86.3	86.3	86.3	86.3	86.3	86.4	86.4	86.4	86.5	86.6	0.4
150.0	86.0	86.0	86.0	86.0	86.1	86.0	86.0	86.0	86.0	86.1	86.1	86.1	86.2	86.2	0.3
152.0	85.7	85.7	85.8	85.8	85.8	85.8	85.7	85.7	85.8	85.8	85.8	85.8	85.8	85.9	0.3
154.0	85.4	85.4	85.5	85.5	85.5	85.5	85.5	85.5	85.5	85.5	85.5	85.5	85.5	85.7	0.2
154.8	85.3	85.4	85.4	85.5	85.5	85.4	85.4	85.4	85.4	85.4	85.5	85.5	85.5	85.6	0.3

MONITOR WELL NC-13

	10/05/93	11/01/93	12/02/93	1/5/94	2/6/94	03/07/94	04/11/94	05/09/94	08/31/94	12/5/94	03/24/95	09/12/95	10/16/96	Cumul.
Depth	Temp.	Temp.	Temp.	Temp.	Temp.	Temp.	Temp.	Temp.	Temp.	Temp.	Temp.	Temp.	Temp.	Diff.
(m)	(°C)	(°C)	(°C)	(°C)	(°C)	(°C)	(°C)	(°C)	(°C)	(°C)	(°C)	(°C)	(°C)	(°C)
20.0	26.8	26.9	26.7	26.7	26.6	26.6	26.6	26.6	26.5	26.7	26.7	26.4	24.9	-1.9
40.0	40.7	40.8	40.6	40.4	40.3	40.4	40.5	40.5	40.4	40.5	40.4	40.4	40.1	-0.6
50.0	47.4	47.4	47.5	47.3	47.4	47.4	47.6	47.6	47.6	47.8	47.8	47.9	47.9	0.4
52.0		49.0	48.9	48.9	49.0	49.1	49.1	49.2	49.3	49.4	49.5	49.6	49.8	0.8
54.0		50.7	50.6	50.6	50.6	50.7	51.0	50.8	51.0	51.2	51.2	51.3	51.6	0.9
56.0	52.2	52.4	52.3	52.4	52.5	52.5	52.7	52.8	52.8	53.1	53.2	53.3	53.6	1.4
58.0	54.2	54.3	54.3	54.5	54.4	54.5	54.7	54.6	54.9	55.3	55.4	55.4	55.8	1.6
60.0	56.3	56.5	56.5	56.7	56.8	56.8	57.1	57.1	57.2	57.6	57.7	57.9	57.8	1.5
62.0	58.6	58.8	58.8	58.9	59.1	59.1	59.6	59.6	59.6	60.0	59.9	60.1	60.1	1.5
64.0	60.7	61.1	61.1	61.2	61.2	61.5	61.8	61.9	62.0	62.4	62.2	62.2	62.3	1.5
66.0	63.3	63.8	63.9	61.1	64.0	63.9	64.3	64.6	64.7	65.0	64.7	64.7	64.6	1.3
68.0	66.0	66.1	66.1	66.2	66.4	66.4	66.6	67.0	67.4	67.4	67.2	67.2	66.9	0.9
70.0	68.3	68.2	68.3	68.4	68.5	68.6	68.9	68.9	69.6	69.5	69.4	69.5	68.9	0.6
72.0	69.6	69.7	69.8	69.9	70.0	70.2	70.2	70.3	71.3	71.4	71.2	71.3	70.9	1.3
74.0	70.4	70.5	70.6	70.7	70.8	70.9	71.0	71.2	72.2	72.5	72.4	72.5	72.4	2.0
76.0	70.8	70.9	71.1	71.2	71.3	71.4	71.6	71.7	72.6	73.1	73.1	73.3	73.4	2.7
78.0	71.3	71.4	71.5	71.7	71.8	71.9	72.1	72.0	72.8	73.3	73.5	73.7	74.0	2.7
80.0	71.9	72.1	72.2	72.3	72.4	72.5	72.6	72.6	73.1	73.6	73.8	74.1	74.5	2.6
82.0	72.5	72.6	72.7	72.8	72.9	73.0	73.1	73.1	73.5	73.9	74.0	74.4	74.9	2.4
84.0	72.8	73.0	73.0	73.1	73.2	73.3	73.3	73.4	73.7	74.0	74.2	74.6	75.0	2.2
86.0	73.3	73.4	73.4	73.5	73.6	73.6	73.7	73.7	74.0	74.2	74.4	74.7	75.2	1.9
88.0	73.7	73.8	73.8	73.9	73.9	73.9	74.0	74.0	74.2	74.5	74.6	74.8	75.3	1.6
90.0	74.2	74.2	74.2	74.3	74.3	74.4	74.4	74.4	74.6	74.8	74.8	75.0	75.4	1.2
92.0	74.6	74.6	74.6	74.6	74.6	74.6	74.7	74.7	74.9	75.0	75.0	75.1	75.4	0.9
94.0	74.9	75.0	74.9	74.9	74.9	74.9	74.9	75.0	75.1	75.2	75.2	75.3	75.5	0.6
96.0	75.2	75.3	75.3	75.2	75.2	75.2	75.2	75.3	75.4	75.4	75.3	75.4	75.6	0.3
98.0	75.4	75.4	75.4	75.4	75.4	75.4	75.4	75.4	75.5	75.5	75.4	75.5	75.6	0.2
100.0	75.4	75.5	75.4	75.4	75.4	75.4	75.4	75.4	75.5	75.4	75.4	75.4	75.4	-0.0
102.0	75.4	75.4	75.4	75.4	75.4	75.4	75.3	75.3	75.3	75.4	75.3	75.3	75.2	-0.2
104.0	75.3	75.3	75.3	75.3	75.3	75.3	75.3	75.3	75.2	75.2	75.2	75.1	75.0	-0.3
106.0	75.2	75.2	75.2	75.2	75.2	75.2	75.1	75.2	75.1	75.1	75.1	75.0	74.8	-0.4
108.0	75.1	75.1	75.1	75.1	75.1	75.0	75.0	75.0	75.0	74.9	74.9	74.8	74.7	-0.4
110.0	74.9	74.9	74.9	74.9	74.9	74.9	74.8	74.8	74.8	74.8	74.7	74.7	74.5	-0.4
112.0	74.7	74.7	74.7	74.7	74.6	74.6	74.6	74.6	74.6	74.5	74.5	74.4	74.2	-0.4
114.0	74.3	74.4	74.4	74.4	74.4	74.3	74.3	74.3	74.3	74.2	74.2	74.1	73.9	-0.4
116.0	74.0	74.0	74.0	74.1	74.0	74.0	74.0	74.0	73.9	73.9	73.9	73.9	73.6	-0.4
118.0	73.7	73.7	73.7	73.7	73.7	73.7	73.6	73.7	73.6	73.6	73.6	73.5	73.3	-0.4
120.0	73.4	73.5	73.5	73.4	73.4	73.4	73.4	73.4	73.3	73.3	73.3	73.2	73.1	-0.4
121.0	73.2	73.2	73.2	73.2	73.2	73.1	73.1	73.2	73.1	73.1	73.1	73.0	72.9	-0.3

MONITOR WELL NC-15

	08/31/93	10/6/93	11/02/93	12/03/93	01/06/94	01/06/94	03/07/94	04/11/94	05/9/94	08/30/94	12/6/94	03/23/15	09/11/95	10/16/96	Cumul.
Depth	Temp.	Temp.	Temp.	Temp.	Temp.	Temp.	Temp.	Temp.	Temp.	Temp.	Temp.	Temp.	Temp.	Temp.	Diff.
(m)	(°C)	(°C)	(°C)	(°C)	(°C)	(°C)	(°C)	(°C)	(°C)	(°C)	(°C)	(°C)	(°C)	(°C)	(°C)
20.0	37.5	36.6	35.4	36.2	33.5	34.4	37.1	36.2	35.2	36.9	34.8	34.4	37.2	36.0	-1.5
40.0	58.5	58.2	57.8	57.6	58.0	56.8	58.2	57.3	57.3	56.5	58.0	56.5	56.7	56.6	-1.9
50.0	69.6	69.6	69.6	69.3	69.7	69.2		69.2	69.3	68.9	69.6	69.6	68.7	69.8	0.2
52.0	71.3	71.7	71.5	71.4	71.8	71.8	71.9	71.1	71.4	71.2	71.6	71.4	70.8	70.9	-0.3
54.0	73.0	73.8	73.2	72.9	73.6	73.3	73.7	73.0	72.7	72.3	73.3	72.7	72.1	72.1	-0.9
56.0	74.2	75.1	74.6	74.4	74.5	74.5	75.1	74.1	74.5	73.6	73.5	73.6	73.1	73.1	-1.1
58.0	74.5	76.1	75.9	75.6	75.6	75.7	76.4	75.1	75.3	74.4	74.2	74.3	73.6	73.8	-0.6
60.0	77.0	77.2	77.2	77.3	75.2	75.2	76.1	75.2	75.4	74.8	74.7	74.8	74.6	75.9	-1.1
62.0	78.2	78.3	78.3	78.4	78.7	79.0	79.5	79.9	79.9	77.8	77.7	77.8	77.3	77.6	-0.6
64.0	81.8	81.2	81.5	81.9	82.1	82.1	82.0	82.0	81.9	79.7	79.3	81.2	79.6	78.7	-3.1
66.0	82.4	82.5	82.6	82.6	82.5	82.5	82.3	82.3	82.1	82.1	82.1	82.3	81.9	81.1	-1.4
68.0	82.6	82.7	82.8	82.8	82.8	82.7	82.6	82.5	82.4	82.4	82.6	82.5	82.2	81.9	-0.7
70.0	82.9	83.0	83.0	83.1	83.0	82.9	82.8	82.8	82.6	82.6	82.8	82.7	82.4	82.2	-0.7
72.0	83.2	83.3	83.3	83.3	83.4	83.2	83.2	83.1	83.0	82.9	83.1	82.9	82.7	82.6	-0.7
74.0	83.5	83.6	83.7	83.7	83.6	83.6	83.5	83.4	83.3	83.2	83.4	83.3	83.0	82.9	-0.6
76.0	83.8	83.9	83.9	84.0	84.0	83.8	83.8	83.7	83.6	83.4	83.7	83.7	83.4	83.2	-0.6
78.0	84.1	84.1	84.2	84.2	84.2	84.1	84.0	83.9	83.8	83.7	83.9	83.8	83.6	83.4	-0.6
80.0	84.2	84.3	84.4	84.4	84.4	84.2	84.2	84.1	84.0	83.9	84.1	84.0	83.8	83.6	-0.6
82.0	84.4	84.4	84.5	84.6	84.5	84.4	84.3	84.3	84.2	84.0	84.4	84.2	84.0	83.8	-0.6
84.0	84.6	84.6	84.7	84.7	84.7	84.6	84.5	84.5	84.4	84.2	84.4	84.4	84.1	84.0	-0.6
86.0	86.4	86.5	86.7	86.8	86.8	86.7	86.6	86.6	86.4	85.8	86.3	86.4	85.9	85.7	-0.8
88.0	88.0	88.0	88.2	88.2	88.2	88.1	88.1	88.1	88.0	87.3	87.8	87.9	87.4	87.2	-0.7
90.0	88.9	89.0	89.0	89.1	89.1	89.1	89.0	89.0	89.0	88.5	88.7	88.8	88.5	88.2	-0.7
92.0	89.5	89.5	89.6	89.6	89.6	89.6	89.5	89.5	89.5	89.4	89.4	89.4	89.2	89.1	-0.5
94.0	89.8	89.8	89.9	89.9	89.9	89.9	89.8	89.8	89.8	89.7	89.8	89.7	89.6	89.5	-0.4
96.0	90.1	90.1	90.1	90.1	90.2	90.1	90.1	90.1	90.0	90.0	90.0	90.0	89.8	89.8	-0.3
98.0	90.2	90.2	90.2	90.3	90.3	90.3	90.2	90.2	90.2	90.2	90.2	90.2	90.0	90.0	-0.2
100.0	90.4	90.4	90.4	90.5	90.5	90.4	90.4	90.4	90.4	90.4	90.4	90.4	90.3	90.2	-0.1
100.3	90.4	90.4	90.4	90.5	90.5	90.4	90.4	90.4	90.4	90.4	90.4	90.4	90.3	90.2	-0.1

MONITOR WELL NC-7

	08/31/93	10/06/93	11/2/93	12/02/93	1/5/94	2/7/94	03/08/94	04/11/94	05/10/94	08/31/94	12/06/94	03/23/95	09/11/95	10/16/96	Cumul.
Depth	Temp.	Temp.	Temp.	Temp.	Temp.	Temp.	Temp.	Temp.	Temp.	Temp.	Temp.	Temp.	Temp.	Temp.	Diff.
(m)	(°C)	(°C)	(°C)	(°C)	(°C)	(°C)	(°C)	(°C)	(°C)	(°C)	(°C)	(°C)	(°C)	(°C)	(°C)
20.0	22.6	22.8	22.2	22.1	22.0	21.7	21.9	22.9	22.6	24.7	21.3	22.3	24.8	24.3	1.7
40.0	29.8	30.0	29.5	29.4	29.5	30.1	29.6	30.0	29.8	29.6	29.0	29.4	30.0	30.1	0.3
60.0	35.6	35.6	35.4	35.7	35.5	35.9	35.7	35.9	36.0	35.4	35.3	35.4	35.6	35.6	0.1
66.0	36.9	36.9	36.9	36.9	36.9	36.9	36.9	36.9	36.9	36.9	36.8	36.8	36.7	37.1	0.2
68.0	37.2	37.3	37.3	37.3	37.3	37.3	37.3	37.2	37.3	37.2	37.2	37.2	37.1		-0.1
70.0	37.6	37.7	37.6	37.7	37.6	37.7	37.6	37.6	37.6	37.6	37.6	37.6	37.5	37.5	-0.1
72.0	38.0	38.0	38.1	38.1	38.0	38.1	38.0	38.0	38.0	38.0	38.0	38.0	37.9	37.9	-0.2
74.0	38.5	38.5	38.5	38.5	38.5	38.5	38.5	38.5	38.5	38.4	38.4	38.4	38.3	38.3	-0.2
76.0	38.8	38.9	38.9	38.9	38.9	38.9	38.9	38.9	38.9	38.8	38.8	38.8	38.7	38.7	-0.2
78.0	39.2	39.2	39.3	39.3	39.3	39.3	39.2	39.3	39.2	39.1	39.2	39.2	39.1	39.0	-0.2
80.0	39.9	40.0	40.0	40.0	40.0	40.0	39.9	39.9	39.9	39.9	39.9	39.9	39.8	39.8	-0.2
82.0	40.6	40.6	40.6	40.6	40.6	40.6	40.6	40.6	40.6	40.5	40.5	40.5	40.4	40.4	-0.2
84.0	41.2	41.2	41.2	41.2	41.2	41.2	41.2	41.2	41.2	41.1	41.1	41.1	41.0	41.0	-0.2
86.0	41.7	41.7	41.7	41.7	41.7	41.7	41.6	41.7	41.7	41.6	41.6	41.6	41.5	41.5	-0.2
88.0	42.1	42.1	42.1	42.1	42.1	42.1	42.1	42.1	42.1	42.0	42.0	42.0	42.0	41.9	-0.2
90.0	42.5	42.5	42.5	42.5	42.5	42.5	42.5	42.5	42.5	42.4	42.4	42.4	42.3	42.3	-0.2
91.0	42.6	42.7	42.7	42.7	42.6	42.7	42.7	42.7	42.7	42.6	42.5	42.5	42.5	42.5	-0.1

MONITOR WELL NC-9

	08/31/93	10/06/93	11/01/93	12/2/93	1/5/94	2/7/94	03/08/94	04/12/94	05/10/94	08/31/94	12/6/94	03/24/95	09/12/95	10/17/96	Cumul.
Depth	Temp.	Temp.	Temp.	Temp.	Temp.	Temp.	Temp.	Temp.	Temp.	Temp.	Temp.	Temp.	Temp.	Temp.	Diff.
(m)	(°C)	(°C)	(°C)	(°C)	(°C)	(°C)	(°C)	(°C)	(°C)	(°C)	(°C)	(°C)	(°C)	(°C)	(°C)
20.0	23.2	23.1	22.8	22.7	23.1	22.0	21.7	22.6	23.0	24.0	22.6	22.5	22.8	22.3	-0.8
40.0	32.9	33.0	32.3	32.7	32.5	32.2	32.7	32.3	32.2	32.2	31.9	31.7	31.4	31.3	-1.6
60.0	42.5	42.7	41.9	42.6	41.6	42.0	42.9	41.8	42.0	41.6	41.6	41.2	40.9	40.8	-1.7
70.0	46.4	46.3	45.8	45.9	45.4	45.4	45.6	45.7	45.8	45.6	45.6	45.6	45.1	44.8	-1.6
72.0	47.3	47.0	47.0	46.9	46.7	46.7	46.8	47.0	46.8			46.5			-0.8
74.0	48.0	47.8	47.9	47.9	47.8	47.7	47.8	47.8	47.7	47.4	47.2	47.3	47.0	46.5	-1.5
76.0	48.7	48.5	48.6	48.6	48.5	48.5	48.5	48.6	48.4	48.0	48.0	48.1	47.8	47.2	-1.4
78.0	49.4	49.3	49.3	49.3	49.3	49.3	49.3	49.3	49.2	48.8	48.7	48.8	48.5	47.9	-1.5
80.0	50.2	50.1	50.1	50.1	50.1	50.0	50.1	50.1	50.0	49.6	49.5	49.6	49.3	48.7	-1.5
82.0	50.9	50.9	50.9	50.9	50.8	50.8	50.8	50.8	50.7	50.4	50.3	50.4	50.1	49.5	-1.5
84.0	51.7	51.6	51.7	51.6	51.6	51.6	51.5	51.6	51.5	51.1	51.1	51.1	50.8	50.2	-1.5
86.0	52.3	52.2	52.3	52.3	52.2	52.2	52.2	52.2	52.1	51.9	51.8	51.8	51.5	50.9	-1.4
88.0	52.9	52.9	52.9	52.9	52.8	52.8	52.8	52.8	52.7	52.5	52.4	52.4	52.1	51.6	-1.3
88.9	53.1	53.1	53.1	53.1	53.1	53.1	53.0	53.0	53.0	52.7	52.7	52.6	52.3	51.9	-1.3